GEOMAR REPORT

GEOMAR

Helmholtz-Zentrum für Ozeanforschung Kiel

RV POSEIDON
Fahrtbericht / Cruise Report
POS469

02. – 22.05.2014
(Bari, Italy – Malaga, Spain)

"PANAREA"

Panarea shallow-water diving campaign
10. – 19.05.2014

Berichte aus dem GEOMAR
Helmholtz-Zentrum für Ozeanforschung Kiel

Nr. 19 (N. Ser.)

Oktober 2014

GEOMAR

Helmholtz-Zentrum für Ozeanforschung Kiel

RV POSEIDON
Fahrtbericht / Cruise Report
POS469

02. – 22.05.2014
(Bari, Italy – Malaga, Spain)

"PANAREA"

Panarea shallow-water diving campaign
10. – 19.05.2014

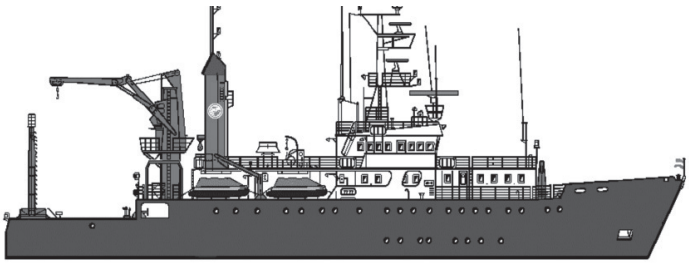

Berichte aus dem GEOMAR
Helmholtz-Zentrum für Ozeanforschung Kiel

Nr. 19 (N. Ser.)

Oktober 2014

ISSN Nr.: 2193-8113

GEOMAR
Helmholtz-Zentrum für Ozeanforschung Kiel

Das GEOMAR Helmholtz-Zentrum für Ozeanforschung Kiel ist Mitglied der Helmholtz-Gemeinschaft Deutscher Forschungszentren e.V.

The GEOMAR Helmholtz Centre for Ocean Research Kiel is a member of the Helmholtz Association of German Research Centres

Herausgeber / Editor:
Peter Linke and Shipbord scientific party

GEOMAR Report
ISSN Nr. 2193-8113, DOI 10.3289/GEOMAR_REP_NS_19_2014

Helmholtz-Zentrum für Ozeanforschung Kiel / Helmholtz Centre for Ocean Research Kiel
GEOMAR
Dienstgebäude Westufer / West Shore Building
Düsternbrooker Weg 20
D-24105 Kiel
Germany

Helmholtz-Zentrum für Ozeanforschung Kiel / Helmholtz Centre for Ocean Research Kiel
GEOMAR
Dienstgebäude Ostufer / East Shore Building
Wischhofstr. 1-3
D-24148 Kiel
Germany

Tel.: +49 431 600-0
Fax: +49 431 600-2805
www.geomar.de

Table of contents

1 Introduction

Peter Linke, Stefan Sommer, Mark Schmidt

Natural discharge of gases such as methane but also higher hydrocarbons from the seafloor is a worldwide phenomenon and is related to a variety of different geological settings such as cold seeps at active or passive margins, mud volcanisms, hydrothermal vents or submarine volcanic exhalations. Gas emissions caused by man-made activities are related to offshore gas and oil exploration. In recent years, the sub seabed storage of carbon dioxide within the Carbon capture and storage technology (CCS) has been discussed as a short-term approach to mitigate climate change caused by anthropogenic emissions of carbon dioxide (CO_2). This involves the capture of CO_2 emitted from large point sources and its injection into deep geological reservoirs, such as depleted hydrocarbon reservoirs and deep saline aquifers, both on land and offshore. The Sleipner project, in the North Sea, is the world's first and largest offshore CCS project, where about 1 million tons of CO_2 are injected per year into the Utsira sandstone formation. With regard to oil and gas exploration as well as CCS technology there is increasing political and societal pressure to develop suitable monitoring strategies allowing the safe operation of offshore installations and methodologies to determine the source strength of gas release in case of leakage events.

Although gas ebullition can be easily detected using hydro-acoustical methods, the quantitative determination of the source strength is still difficult to constrain. Vigorous gas release is associated with plume formation and complex water transport that also affects the distribution of other gases that are dissolved in the seawater (N_2, O_2, Ar) in the near and far field of such sites (McGinnis et al., 2004). The characterization of the dynamics of buoyant plumes produced by a source of bubbles in a liquid is relevant in several contexts including that of the analysis of natural gas discharge, underwater blowouts as well as engineering disciplines like destratification of reservoirs (Espa et al., 2010) or safe employment and monitoring of submarine CO_2 storage sites. A current interest has developed on the study of CO_2 plumes in the marine realm as a natural analogue for the effect of leakages from sub-seabed CO_2 sequestration sites (Espa et al., 2010). Several bubble release experiments have been conducted at a laboratory scale or in shallow lacustrine settings (McGinnis et al., 2004) to investigate the behaviour of bubble plumes in stratified and un-stratified environments. It is aimed to use numerical models to simulate bubble dissolution and plume dynamics in order to determine the source strength of gas emission sites. However, validation of numerical models with marine field data is still rare.

According to the plume model theory (detailed by Espa et al., 2010, McGinnis et al., 2002, 2004, 2011, and Wüest et al., 1992) a two phase plume of water and gas is created by the upwelling and entrainment of water, which is induced by the buoyancy increase, due to sufficient and rapid gas release at the seabed. In regard to a stratified water column, bubbles within the inner plume core transport denser liquid upward and entrain surrounding seawater, which results in a destratification and intense mixing of the water column.

At a certain level some water is again detrained from the core to balance buoyancy and spread horizontally (Espa et al., 2010). Moreover, temperature and salinity gradients, which might occur in the water column, can act as boundary layer for plume buoyancy, resulting in a widespread horizontal dispersion of plume water along this threshold. As the plume rises, the bubbles dissolve into the ambient and entrained water, decreasing both the bubble driven buoyancy and the concentration gradient along the bubble water interface. Depending on their initial bubble size, pure CO_2 bubbles mostly dissolve within the first meters upon release. Due to the concentration gradient at the bubble-water interface other dissolved gases (mostly N_2 and O_2) are stripped from the seawater into the bubble, while the CO_2 is being dissolved. Beside the local risk of seawater acidification, this implicates a risk of oxygen depletion in bubble influenced regions. When nearly all CO_2 is dissolved, the gases that were previously stripped begin to re-dissolve and the N_2:O_2 mole fraction reaches atmospheric levels (McGinnis et al, 2010).

Due to the rapid dissolution of CO_2 bubbles (CO_2 is 25 to 30 times more soluble in seawater than CH_4) a CO_2 plume will lose buoyancy quickly and the plume water tends to sink downward (fall back water),

because the density of CO_2-enriched seawater increases (McGinnis et al., 2011). This results in the tendency of CO_2-rich water to remain at or to sink to the seafloor (McGinnis et al., 2011 and references cited therein). Such conditions could especially affect the local benthic environment, mostly due to the lowering of the pH. Knowledge of the bubble-plume-seawater interaction is thus essential to correctly simulate bubble dissolution and plume dynamics, which control the dispersion of dissolved CO_2 and other dissolved gases in the near- field water column.

POSEIDON cruise POS469 to the submarine volcanic gas discharge sites off Panarea (Aeolian Islands, South Italy) was conducted within the framework of the ECO2 project (EU) and the Helmholtz-Alliance "ROBEX – Robotic Exploration of Extreme Environments". The Panarea gas vents represent a unique environment as carbon dioxide (CO_2), methane (CH_4), hydrogen (H_2), nitrogen (N_2), helium (He) as well as hydrogen sulfide (H_2S) is simultaneously emitted into the water column. This and the different source strengths of gas discharge render the Panarea area an ideal test bed for the study of the dynamics of gas discharge and associated plume formation.

The major aim of the cruise was to quantitatively understand the dynamics of plume formation and its effects on the distribution of different gases dissolved in the ambient seawater applying appropriate plume models that enable the determination of the source strength of the respective gas discharge site. Under consideration of bubble rise velocity and bubble size, the models will be parameterized and validated by gas measurements of pCO_2, CH_4, H_2S, N_2, oxygen (O_2), and argon (Ar) conducted in the surrounding of gas discharge. Gases were simultaneously measured using the prototype of a novel Underwater Membrane Inlet Mass Spectrometer (MIMS). Investigations will be conducted along transects across discharge sites using the ROV PHOCA and a towed video-guided pump CTD. In parallel to these ship based deployments, measurements were conducted by divers at the shallow gas vents off Panarea Island.

Panarea, located in the southern Tyrrhenian Sea, is the smallest island of the Aeolian volcanic arc, which comprises seven major islands and a number of submerged volcanoes extending for approximately 200 km parallel to the continental slope of northern Sicily and western Calabria (Beccaluva et al., 1985). Volcanism started 1.5 Ma ago and is related to the subduction of the African continental plate below the Eurasian plate (Esposito et al, 2006; Dekov & Savelli, 2004). The island of Panarea rises from the western sector of a 56 km^2, near-circular submarine platform that occurs at a water depth of 120 m. This platform is the flat, eroded summit of a large submarine stratovolcano that is over 1,500 m in height (Gabbianelli et al. 1990; Favalli et al. 2005).

Submarine venting of gas and thermal waters is widespread at the summit platform of Panarea and has been known since early historical times (Italiano & Nuccio, 1991; Calanchi et al., 1995; Esposito et al., 2006). Present day volcanic activity is most prominently revealed by frequent eruptions of lava at the Stromboli volcano and extensive fluid exhalations on top of the plateau to the east of Panarea Island (Anzidei et al., 2005) in the area of the central islets Dattilo, Panarelli, Lisca Bianca, Bottaro, and Lisca Nera. In this area, numerous gas vents occur at water depths ranging from 5 to 35 m (Anzidei et al., 2005) releasing mainly CO_2 and a small fraction of N_2, H_2S, He, H_2 and CH_4 (Caracausi et al., 2005, Chiodini et al. 2006). The CO_2-rich gas emissions originate from a geothermal reservoir that is fed by magmatic fluids derived from an actively degassing melt or a cooling magmatic body (Italiano and Nuccio 1991; Caracausi et al. 2005). Whereas these shallow gas discharge sites are well known, only recently further gas discharge sites at about 70 – 80 m water depth were discovered during a cruise with RV Urania in 2011 (McGinnis et al., 2011) and a previous cruise with RV Poseidon in 2006 (Monecke et al., 2012). Acoustic evidence of rising gas bubbles (flares) at about 80 different locations and elevated surface concentrations in methane and carbon dioxide were found throughout the surveyed area (Fig. 1).

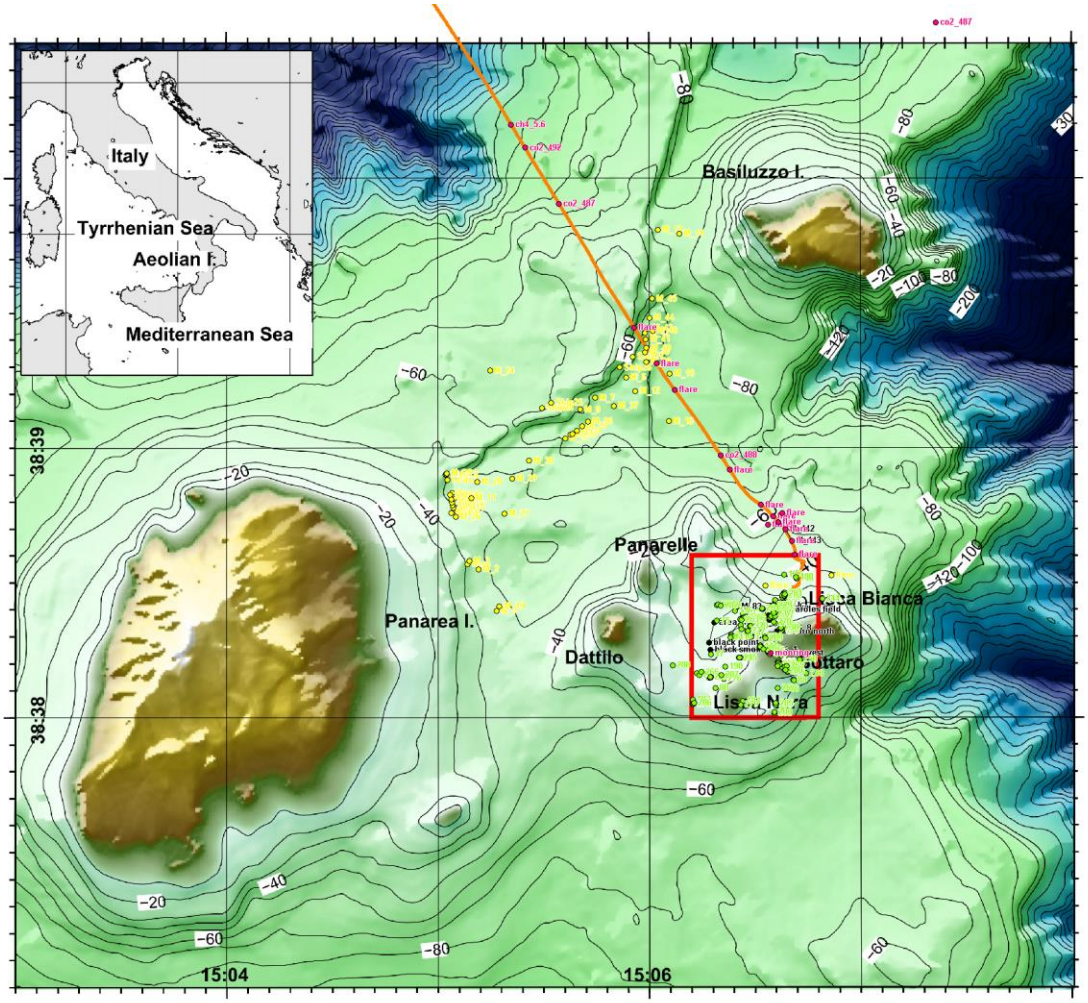

Fig. 1: Map of the working area at the gas discharge sites off Panarea (Aeolian Archipelago, South Italy). Occurrence of deeper gas discharge discovered during the RV Urania cruise (McGinnis et al., 20111) is shown by yellow dots, shallow gas release sites are indicated by the red rectangle. Figure adapted from Aliani et al. (2010).

The flares either plot aligned to a morphological structure in the northwest of the plateau or in clusters. Due to different kinds of gas release and its specific gas composition co-occuring at the seafloor off Panarea encompassing diffuse gas release, vigorous gas emissions producing bubble plumes, and single bubble streams of varying strength, this is a unique and excellent area to study possible leakage scenarios of various manner and strength and represents an ideal test bed for our novel UW MIMS.

2 Cruise Narrative

Peter Linke

Tue. 29.04.: At 19:00 (LT) the scientific crew arrived in Bari and was transferred to the Hotel „Boston“. A reception of local authorities and VIPs on board of RV Poseidon was conducted with participation of Mark Schmidt, Jens Schneider von Deimling, Steffen Aßmann, and Stefan Sommer.

Wed. 30.04.: 08:00 Pick up of scientific crew at the Hotel and transfer to the ship. Start with loading activities of scientific equipment and the ROV, establishment of the laboratories.

Thu. 01.05.: Establishment of laboratories. In the afternoon the harbour test of the ROV was conducted successfully. 17:30 Arrival of Boris Schulze (L-3 Communications ELAC Nautik GmbH).

Fri. 02.05.: We left the harbour of Bari at 10:20, weather conditions were nice and sea was calm. Transit was used for tests of the mass spectrometer and TA device as well as for ROV maintenance. Underway tests of the multibeam system were conducted.

Sun. 04.05.: Station work started with a vertical CTD-cast to obtain physical data (e.g. sound velocity) for calibration of the multibeam system and a first set of water samples from the working area. This was followed by a first multibeam transect east off Panarea Island followed by a second profile towards Stromboli volcano into deeper waters.

Mon. 05.05.: In the morning, a first transect with the video pump CTD was conducted before the vessel went on transit to Milazzo for the exchange of Boris Schulze against Peter Linke by boat transfer off port limits. After this, the vessel headed back towards Panarea where a surface water transect with the Total Alkalinity (TA) system was performed. During the evening and night several multibeam, water column imaging (WCI) and ADCP profiles were conducted in parallel to look in the south of the shallow plateau for gas flares and potential targets for the ROV and pump CTD. RV Urania showed up in the working area.

Tue. 06.05.: Unfortunately, the first ROV station had to be abandoned due to technical problems with the ship's data protocol. Instead, the video pump CTD was towed in bottom view along the profiles where flares had been detected before. During this transect we discovered at least 3 areas with rising gas bubbles and strong chemical anomalies. This long transect was followed by a multibeam survey.

Wed. 07.05.: The second ROV dive repeated the previous pump CTD survey and we discovered some small chimneys with shimmering water and we were able to fill the gas sampler at a site with moderate gas flow and single gas outlets. Just when we arrived at a larger gas venting patch we had to abandon the dive due to a ground fault alarm in the telemetry. However, after a rapid retrieval of the ROV and opening of the telemetry cylinder it became apparent that the sensor had been turned loose and got connected to the housing. After putting the sensor back into position we were able to perform a second dive at the position where the previous dive had ended. We took a gas sample and 2 Niskin water samples at the gas venting patch, which was named "whirl pool". We continued the dive along the small volcanic ridge to the east and discovered a strong gas venting activity in a crater at 70m water depth within a rough topography. When diving here, the captain of the Italian RV Urania came very close to Poseidon and asked us how long we would stay at this position. The ROV dive followed a multi beam transect to Stromboli where we mapped the area near Strombolichi, the ancient magma channel of the volcano.

Thu. 08.05.: ROV dive 4 was very short and just to deploy an ADCP on a flat and sandy area between 2 gas vent fields. During the following pump CTD we conducted a dense grid in 3 depth layers above the 1st vent site to monitor the lateral and vertical spreading of the chemical signals. After this, a multibeam, WCI and ADCP survey was conducted at the western side of Panarea Island.

Fri. 09.05.: During ROV dive 5 the bubble box was deployed at the 1st vent field on top of vents with single gas streams to measure the bubble size, rise velocity and discharge rate. After this, a short multibeam profile was done across the whirl pool site to produce a grid for towing the pump CTD in 3 different depth layers. Afterwards, a multibeam and WCI survey was conducted south of the shallow plateau.

Sat. 10.05.: During ROV dive 6 the bubble box was used to measure the bubble size and discharge rate at the whirl pool site and another gas sampler was filled for on board GC analysis. The following video pump CTD was towed in 3 depth layers at the strong vent site to measure the lateral and vertical extent of the chemical signal of this vent. After this we headed for Stromboli to conduct another multibeam, WCI and ADCP survey on the western flank of the volcano.

Sun. 11.05.: As RV Urania had left the working area and the local fisher had removed their boat, we were able to fill the gas sampler and 3 Niskin samples at "strong vent" during ROV dive 7. After this, the zodiac of the diver team came by to pick up their equipment and to talk about the sampling strategy during the coming days. In the afternoon we used the ship's zodiac to visit the strong gas vents east off

Bottaro Island, which were too shallow for Poseidon (Fig. 2). Here, we took gas and water samples and obtained underwater video. After this, we continued the multibeam survey south of the shallow Panarea plateau.

Fig. 2: View on islands Stromboli and Bazilluzzo with RV Urania (left) and surface expression of the strong gas discharge near Bottaro Island with Islands Salina (far left), Panarea and Datillo.

Mon. 12.05.: During ROV dive 8 the bubble box was deployed at the whirl pool site to conduct a stain release experiment. Furthermore, the ROV's sonar was used to trace the rising gas bubbles during their ascent through the water column. After this, the video pump CTD was towed in 2 additional depth layers at the grid of the strong vent. This was followed by two CTD stations forming a grid of 9 vertical casts around the "strong vent". A multibeam survey was used to close gaps in the existing data set.

Tue. 13.05.: During ROV dive 9, the second ADCP was deployed next to the crater with the strong vent, where later a stain release experiment and vertical sonar mapping of the rising gas bubbles was performed. After transit to a second crater we found a large lobster trap and bubbling vents in the center of the depression with the highest CO_2-concentrations of the cruise. However, when we tried to conduct a grid with the video pump CTD, the ship had to manoeuver around buoys with fish lines, bringing the CTD close to the steeply rising slope. Therefore, we had to abandon this deployment. The last multibeam survey was used to complete the existing data set.

Wed. 14.05.: During the night, the wind had peaked up and we went on transit towards Milazzo. Unfortunately, the harbor master closed the harbor due to the upcoming storm and we had to change plans and asked for the transfer of scientists (Steffen Aßmann, Jens Schneider v. Deimling, and Stefan Sommer in exchange for Nadja Kinski) off Messina harbor limits by boat shuttle, where the vessel arrived at 13:00. After the transfer the vessel headed back to Panarea Island against strong wind and waves, where we arrived in the early morning.

Thu. 15.05.: Strong wind and swell limited the use of our instrumentation, but we were able to recover both ADCPs during ROV-dives 10 and 11 in the afternoon as the weather predictions did not show any improvement for the 2 coming days.

Fri. 16.05.: In the morning, we were facing thunderstorms and strong winds with rain from different directions. When the weather calmed down a bit, a boat transfer was conducted bringing Maike Nicolai to the vessel. During ROV-dive 12 to the whirl pool site the bubble box measurements and the stain release experiment were repeated, followed by a grid of 9 vertical CTD casts around the whirl pool. After this, the equipment of the divers was brought back to the vessel and Maike Nicolai was taken on the zodiac to accompany diving at the shallow sites. After their dive, gas samples were transferred for GC analysis on board and we gave a farewell to the diving team (Fig. 3). The vessel left the working area at 18:25 for transit to Malaga, Spain. However, the transit was used for a continuous TA measurement of the surface waters and for analysis of the gas samples (Fig. 4).

Thu. 22.05.: The transit ended after a stormy night at 08:00 at the pilot station off Malaga. The vessel was guided into the harbor and demobilization started after custom clearance with the unloading of the

ROV-container and dismantling of the ROV launch and recovery system at the vessel's A-frame. After this, boxes and other equipment were craned ashore and transferred on a truck. The scientific crew disembarked at 14:30 with cheerful thanks to the captain and crew of RV Poseidon.

Fig. 3: Farewell to the diving team after exchange of equipment and samples.

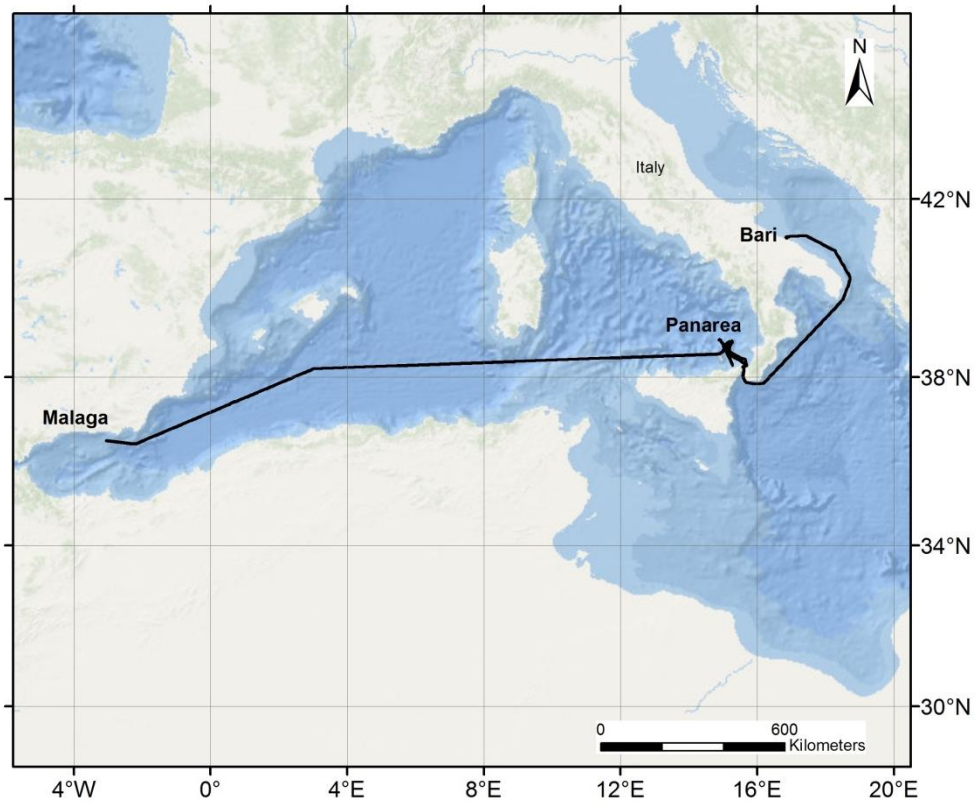

Fig. 4: Overview of cruise track POS469 starting from Bari (Italy) finishing in Malaga (Spain). The long transit from Panarea to Malaga was used for continuous Total Alkalinity (TA) measurements and standard oceanographic parameters of surface water.

3 Participants

	Name	Function	Institute/Company
1	Linke, Peter	Chief scientist, ROV	GEOMAR
2	Sommer, Stefan	Co-PI, MIMS	GEOMAR
3	Schmidt, Mark	CTD, Sensors	GEOMAR
4	Schneider v. Deimling, Jens	Multibeam	GEOMAR
5	Aßmann, Steffen / Kinski, Nadja	TA-Analytik	GEOMAR/CONTROS
6	Cherednichenko, Sergiy	MIMS, Video	GEOMAR
7	Cuno, Patrik	ROV	GEOMAR
8	Pieper, Martin	ROV	GEOMAR
9	Hennke, Jan	ROV	GEOMAR
10	Huusmann, Hannes	ROV	GEOMAR
11	Bodendorfer, Matthias	ROV	GEOMAR
12	Schulze, Boris	Multibeam	L-3 Com. ELAC Nautik
13	Vielstädte, Lisa	Dive PI	GEOMAR
14	Bigalke, Nikolaus	Diver	GEOMAR
15	Howe, Christian	Diver	Submaris
16	Kreutzburg, Matthias	Diver	GEOMAR
17	Nicolai, Maike	Documentation	GEOMAR

4 Methodology and Preliminary Results

4.1 Acoustic and visual gas seepage observations

Jens Schneider v. Deimling

Methodology

Multibeam system description and setup

A fix installation 50 kHz multibeam SB3050 with a 1.5° x 2° TX/RX aperture manufactured by L-3 ELAC Nautik GmbH was used for bathymetric and water column imaging (WCI) surveying during POS469. In single ping mode one transmission cycle is characterized by the formation of three simultaneously yaw and pitch stabilized transmit-sub fans with subsequent roll-stabilization during receive. The center transmit-sub fan has the frequency F1 slightly different from the respective outer sub fans with frequency F2 to foster reception signal separation. The system covers a maximum of 140° swath width. In multi ping mode, a second swath is formed also having three transmit sub fans with frequencies F3 and F4, respectively. 128 transmission and 64 reception staves transmit and record the echo signals, respectively. The transceiver electronic (SEE37) of the SB3050 then performs A/D conversion of the voltage and reception signal processing of the echo time series for further multibeam processing. 4 PCs (one for each frequency F1-F4) perform real-time hybrid time-delay beam forming to generate up to 191 equi-angle beams (or up to 386 equi-distant beams). The beam formed data were processed in the bottom detection algorithm (BDA) and streamed to the “Operator PC” to display and store bathymetric data in the XSE file format and HYPACK/HYSWEEP.

For accurate positioning and ship movement corrections the two Codaoctopus GPS antennas together with their IMU were used. The F180 GPS reference ellipsoid was set to WGS84. Positions and heading (10Hz) as well as roll, pitch and heave data (TSS1, only 25Hz due to limited system performance) were streamed to the multibeam electronics, time tagging was only feasible through a 1Hz $ZDA Signal but not by PPS! Moreover the data format sent by WERUM for the keel sound velocity could not be parsed by the multibeam system throughout the cruise. Instead, values from an up to date vertical sound velocity profile were loaded via Hydrostar for surficial sound speed approximation.

The latest Hydrostar control software V4.0.0 (built 3.348.1.430) was installed (previous installation Version: 3.5.8) now allowing pitch steering manipulation for enhanced bubble detection as suggested in Schneider von Deimling and Papenberg (2012) with data storage in XSE format and three versions of WCI. The data were further streamed to HYPACK/HYSWEEP for online coverage display.

Water column Imaging (WCI)

Besides bathymetric and sidescan data, uncompressed beam formed time series data of each beam were streamed to the "WCI PC" with a maximum sample rate of one half of the pulse length to visualize the water column backscattering data over travel time in each direction. Contrary to first multibeam gas bubble visualizations in Schneider von Deiming et al. (2007) we here analyze the full beam-formed time series of modern multibeam sonar records. The system even offers alternate storage of raw stave data (not beam-formed). Water column imaging and logging was conducted during most surveys in a way not to lose the spatial coherence of potential rising and current-deflected gas bubbles streams (Schneider von Deimling & Papenberg, 2012). If possible, all sounders (navigation sounders, ADCP) of Poseidon were switched off because they were found to significantly interfere with the SB3050. Single ping mode with 1-2Hz and 0.4ms pulse width was chosen for valuable WCI results in shallow water. The transmission source level and receiver gain were set constant to 0 and 23dB, respectively, allowing for later comparison of echo scattering. The water column data were streamed over a gigabit-ethernet controller to the WCI computer. Significant time latency between echo reception and WCI echogram visualization of approximately 10 seconds occurred. However, this delay had no implication on the total data storage and investigations during post-processing.

Bubble Box

For the assessment of bubble size distribution and bubble rise velocity of CO_2 bubbles, a bubble imaging box (B-Box) was constructed at GEOMAR. The B-Box can be used open top or with a closing lid to either allow undisturbed vertical flow-through, or precise flux measurements into predefined capture volumes. The front and sidewalls are made of transparent acrylic glas for ROV video observation, while the backwall is made of a white acryl glass acting as a light diffuser for backlid illumination of the gas bubbles. An adjustable ROV handle bar is mounted to allow for manipulator arm operation by the ROV PHOCA (Fig. 5).

Fig. 5: B-Box in front of the carrier ROV PHOCA.

For quantitative bubble size determination two GoPro Hero^{+} black edition cameras with extra power packs were attached in pressure-resistant POM housings to the B-Box for later stereographic data evaluation. The lenses of these cameras were adjusted prior to the cruise to obtain a narrower field of view fixed at 80° x 60° degrees. The video mode was set to VGA resolution to allow fast 240 frames per second, which is vital to suppress bubble-mediated motion blur.

Data Processing

Bathymetry and Backscatter

Multibeam data were processed and evaluated on- and off-shore using the MBSystem Software, Fledermaus, Hypack/Hysweep, and MATLAB. The raw XSE data were imported with the MBSystem software for processing, pre-filtering, editing and visualization. A pre-filter was applied using MBSystem to remove the soundings outside a standard deviation threshold level, and to get rid of the outermost ten beams from each side of the swath as these were found to be consistently erroneous. In a later step data were evaluated in 3D especially in those areas with extreme slopes, and where gas seepage bubbles further deteriorated the bottom detection. NETCDF grids were created using a median filter with a grid size according to the local water depth and with respect to the 1.5° x 2° antenna beamwidth of the SB3050 on POSEIDON.

Aside from bathymetric measurements the SB3050 records backscatter and sidescan data in the XSE files. Unfortunately, the current version of MBSystem can only access the beam-amplitude data. To get rid of the intrinsic angular response of backscatter amplitude on grazing angle, backscattering intensity over grazing angle tables were generated for 50 successive pings. Then the average angular response of these 50 pings was taken into account considering the beam angle and the local slope of a cleaned bathymetric grid to obtain true grazing angles. The backscatter was then normalized to a reference angle of 30° to efficiently suppress the intrinsic angular response effects and obviously highlights seabed related backscattering features. Finally, histogram equalization was performed to make use of the full range of 8-bit grayscale values for visualization.

WCI

Water column data were processed on-the-fly via the new “range beam stack” function implemented into the new WCIViewer 3.3.6 software developed within SUGAR in cooperation between GEOMAR and

L-3 Communications ELAC Nautik GmbH. This new feature allows identifying gas seepage features online and within a time history of approximately 15 minutes at once which highly facilitates the detection and localization of gas seepages during a survey. Afterwards the data were converted via the GEOMAR in-house conversion tool "wci2gwc" run on LINUX 64bit to generate QPS-IVS GWC file format with a down-sampling factor of 16. The down-sampled dataset enables easy file handling and echogram visualization of the data in the latest FMMidwater 7.3.5 version. The full water column traces (not down-sampled) were converted to GWC for thorough data evaluation after the cruise. Finally the polar multibeam data were exported as cartesian UTM Coordinates and depth values (ZONE 33) and interpolated in 3D using a near neighbor interpolation scheme. The final 3D cube was then sliced in MATLAB to further investigate the sonar data.

Preliminary Results

The overall goal of the acoustic work during this cruise was not to assess a new bathymetric chart about the well mapped area (Anzidei et al., 2005). Aim of this study was to confirm, refine, and extent earlier findings reported in McGinnis et al. (2011) about 60 m high rising natural CO_2 gas bubbles some nautical miles distant to the Panarea shallow bubbling plateau.

Multibeam calibration

After manual input of static offsets into the F180 setup, the IMU system was successfully calibrated during the transit and reported reasonable values for GPS antenna and baseline orientation offsets. The final attitude and positioning data were well within specification.

After gathering a CTD-derived sound velocity profile in the beginning of the cruise, survey lines were run around 80m water depth within a plane area, and across a steep edge on the seabed, to meet the requirements for a full patch test including ROLL, PITCH, YAW, and LATENCY evaluation. The well-suited calibration survey area gave rise to a successful patch test and the resulting offsets (Tab. 1) were applied for all data recorded later than 5th of May in both, Hydrostar and Hypack/Hysweep.

Table 1: HSO calibration offsets gathered during POS469. X denotes across track, Y along track distance (m), Z is vertical offset (m), TD is time delay (s). The respective reference point was defined as the position of the MRU projected on to the water level. GPS position data were output for the MRU position instead of the position of the primary antenna (Nav. Sensor = Mot. Sensor position).

Nav. Sensor	*Mot. Sensor*	*Hydrophone*	*Projector*
X=0	*X=0*	*X=-1.5*	*X=-1.41*
Y=0	*Y=0*	*Y=6.36*	*Y=5.20*
Z=-5.65	*Z=-5.65*	*Z=4.25*	*Z=4.25*
TD=0		*ROLL=1.45*	*PITCH=-2.40*
			YAW=2.00

Overview survey

Even though the research area was surveyed before by multibeam during various cruises (Anzidai et al., 2005; McGinnis et al., 2011), we re-surveyed the area for the sake of water column imaging and gas seepage detection. Sonar settings were tweaked to highlight water column features which occasionally confused the bottom detection, in turn, WCI performance increased. Nevertheless, bathymetric and WCI data could be acquired at the same time revealing reasonable results.

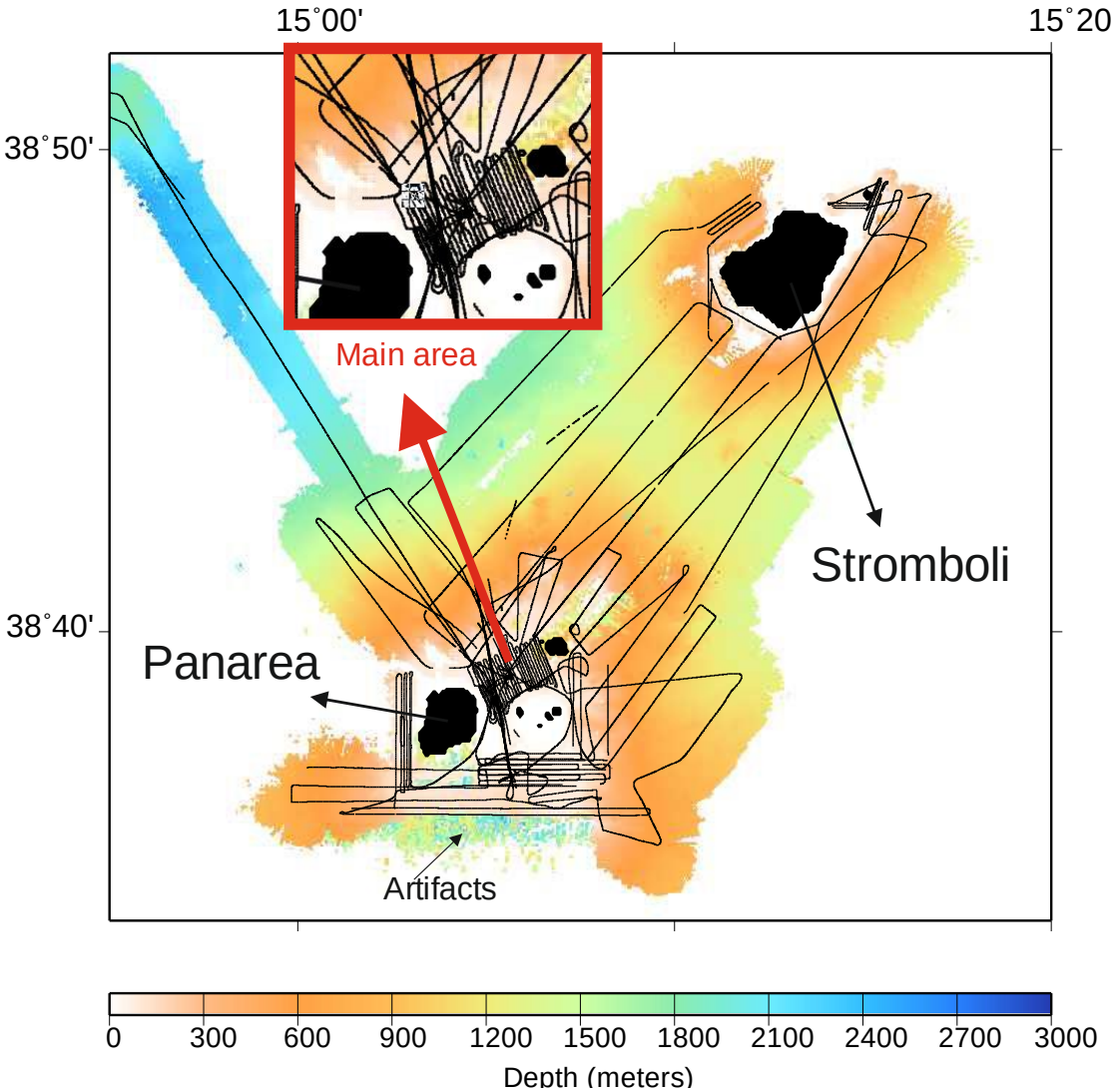

Fig. 6: Overview of all survey lines gathered between 05th and 16th of May using SB3050 Multibeam. The areas cover the flanks of the Panarea (SW) and Stromboli (NE) volcano. The entire survey area was investigated by WCI for identification of potential gas seepage sites. Inlet shows main working area near Panarea.

Figure 6 shows SB3050 data from the research area of POS469 covering water depth between 15 and 2500m. First data analyses reveal that the gas releases are restricted around Panarea to a maximum water depth around 90m. Occasionally, gas bubbles were found to rise as high as 80m up through the water column reaching the transducer depth. Surveys with WCI mode include areas around the Stromboli volcano, but no indications of gas releases were found here. However, the reliability of the first on-the-fly WCI beam stack gas detection was limited, because some data were skipped during the online display due to performance issues (Fig. 7), which had no effect on the recorded data.

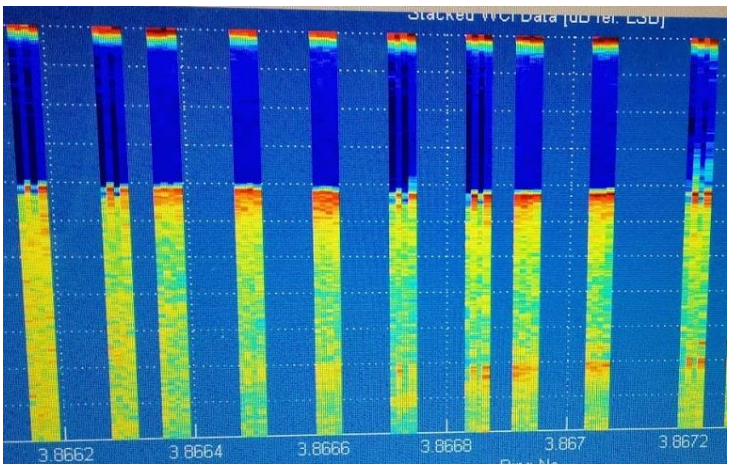

Fig. 7: On-the-fly beam stack echogram visualization revealing regular data gaps due to I/O performance limitation.

So far, only a small fraction of the 1.5 TB of WCI data were analyzed for gas releases. Therefore, we cannot yet totally exclude further gas seepage areas. Consequently, the distribution and occurrence of gas release sites presented in this report denote a preliminary and conservative number.

Local studies at Panarea

Remote acoustic seepage detection

More local acoustic surveying was conducted together with geochemical measurements in the previously found seepage sites (McGinnis et al., 2011) northwest of the well-known shallow seeps east of Panarea. Here, seepage was found to predominantly occur along the WSW-ENE striking ridge (Fig. 8a) and at some places originates out of a depression on the seabed (Fig. 8a, inlet).

Aim of this local survey was to precisely locate and characterize gas seepage sites as a valuable base for succeeding ROV dives and geochemical sampling. Closer analyses of the bathymetry reveals that the most pronounced gas seepages originate from a crater-like 20m wide depression (Fig. 8a) on the seabed that potentially originates from phreatomagmatic explosions in the past. WCI recordings demonstrate that - at least some – gas bubbles rise up to the sea surface (Fig. 8b). This result is in some way contradictory to modeling of medium sized CO_2 bubbles and in situ CO_2 gas release experiments (Linke, 2012), but could be confirmed during an upward moving ROV experiment following gas bubbles from the 60m deep seabed towards the surface (Fig. 9). The most likely explanation for the enhanced uprising and bubble lifetime is the existence of very large bubbles, upwelling, and less likely a varying gas bubble (initial) gas composition.

Apart from the bathymetric depression features, seepage seems to be aligned along the ridge like pattern striking WSW-ENE. No further seabed indications for gas seepage were found. The backscatter generally shows a high variability due to the volcanic nature of the seabed, thus obfuscating potential seepage related backscatter anomalies such as seep related benthic fauna. The low backscattering regime in the southeast of Figure 8d is interpreted as covered by sediments showing homogeneous backscattering behavior.

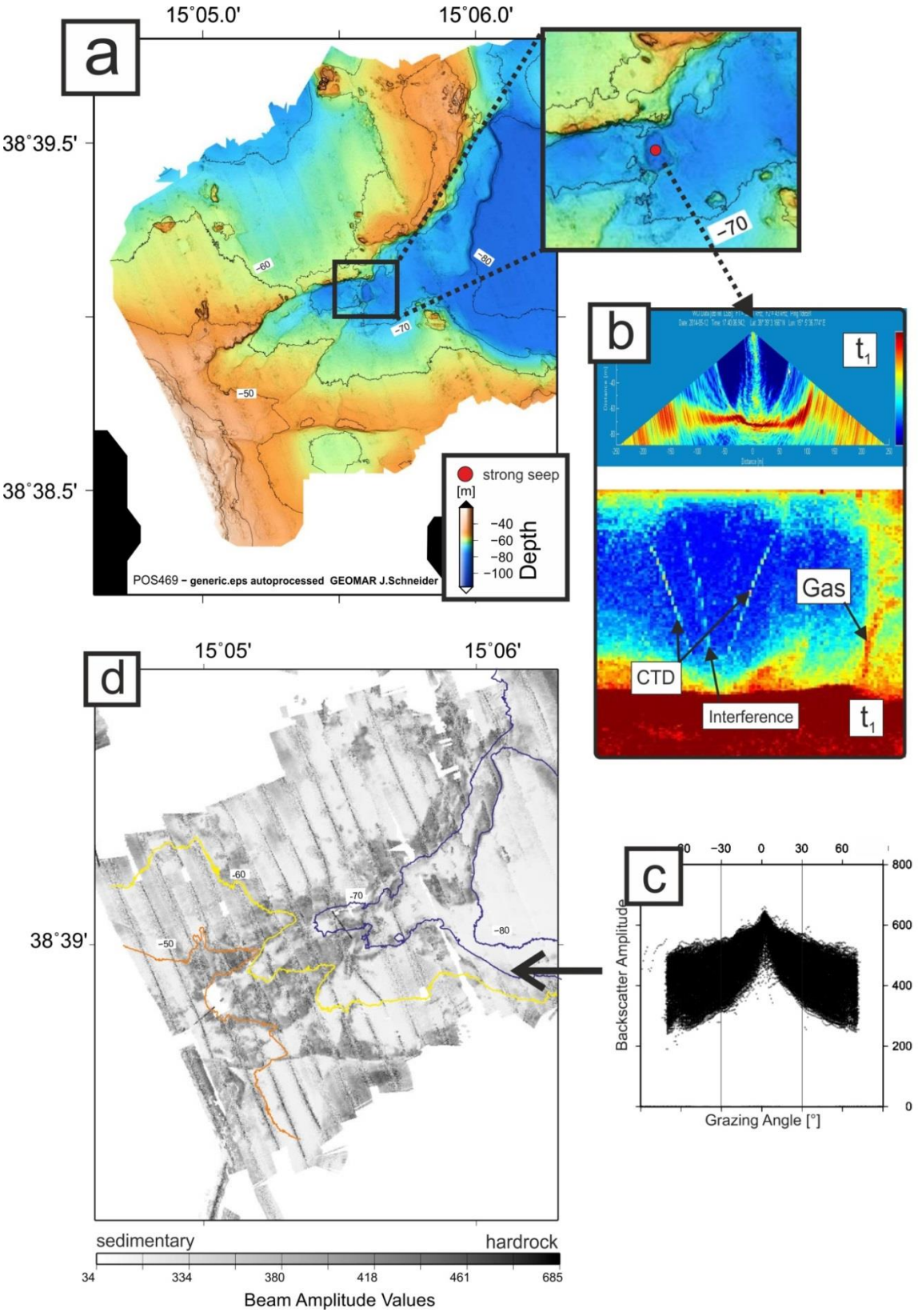

Fig. 8: (a) processed bathymetric grid (3 x 3 m) with histogram-area-equalized color chart revealing volcanic hardrock (brownish) and sediment covered areas (bluish) (b) water column backscattering data in fan snapshot at time t_1 and echogram beam stack view over time with distinct gas release at t_1 from 70 m water depth. CTD down- and upcasts are visible as well as interference echoes from the ship-mounted 75 kHz ADCP (c) example of beam amplitude grazing angle response pattern, that have been used to produce (d) angular-response corrected beam amplitude data with colored depth contour. High backscattering corresponds to rough/volcanic terrain in accordance to (a).

Post-processing of the multibeam water column data allowed for further insight into interior structures of the gas flares. Therefore stationary multibeam data were analysed with a high ping repetition rate. Subsequently, the data were load into MATLAB, threshold- and lowpass- filtered, gridded with a 3D interpolation scheme to obtain a 3D data cube. Individual slices through the 3D cube are presented in Figure 9 revealing interior features like current induced flare deflection and – if successive pings being evaluated over time – revealing vertical rise speed of individual "bubble clusters" as suggested in Schneider von Deimling and Papenberg (2012). Moreover, the general decay of the integrated acoustic energy as a rough indicator for the amount of gas bubbles and respective size distribution across the plume can be assessed by horizontal slices (Fig. 9, inlet).

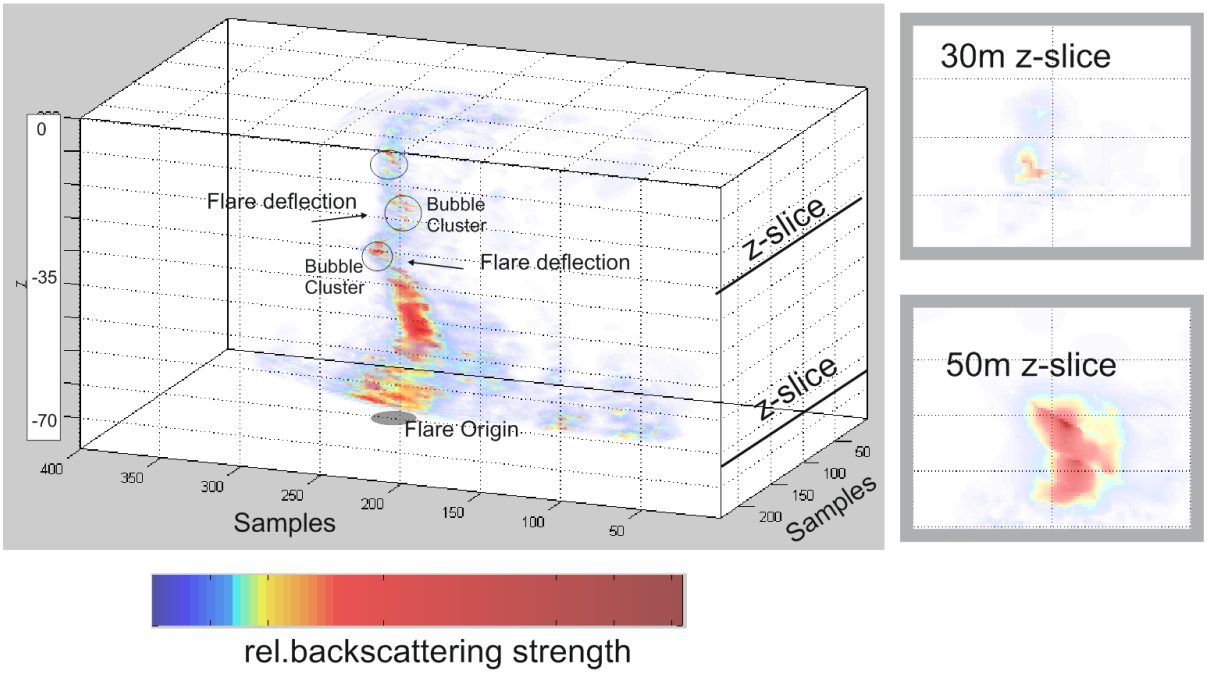

Fig. 9: 3D gridded and filtered data cube from ELAC SB3050 data. One sample is 0.2 m in length. Inlets on the right side represent horizontal slices through the 3D cube for the assessment of plume width and integrated acoustic energy. Plume height achieves 70 m with max with of 6.5 m.

Near range acoustic and visual gas bubble imaging

Acoustic imaging by multibeam sounder clearly revealed that some of the gas bubbles rise up to the sea surface. By using a ROV mounted high frequency sonar this observation was refined and the tempo-spatial evolution and extent of the rising plume could be mapped. Therefore an ROV uplift experiment was conducted. The ROV was positioned 6 m downstream of the gas bubbles. During the first meters of uplift of the ROV pronounced backscatter from the seabed obscured acoustic water column scatterers like gas bubbles. Further upwards and some meters away from the seabed, a very pronounced acoustic signal was acquired and could be clearly cross-linked to the gas seepage site by a downward looking camera. The initial plume dimension could be measured online to 5.3 x 2.9 m at 47 m water depth (Fig. 10a). By slow ROV uplift the bubble plume could be followed from the seabed up to the surface. Meanwhile the acoustic signal strength ceased but maintained up to the sea surface. At 16 m water depth the plume dimension was measured again to 4.3 x 2.0 m (Fig. 10b).

Visually, the gas bubble plume got almost entirely lost only after a few meters of ROV uplift. We conclude that the majority of the gas volume got lost due to dissolution in agreement to Linke (2012). However, a significant fraction of gas obviously survives as bubbles and rises through the water column spanning dozens of meters. This is considered an important finding, because acoustic gas bubble

detection feasibility scales to a certain extent to the bubble rise height: if gas bubbles would rise only 5 m, then acoustic artefacts cannot un-ambiguously be discriminated against such seepages.

Enhanced vertical rise highly increases the acoustic detection feasibility and obviously the amount of remaining gas is high enough for distinct detection (Fig. 10b). Thus, even though bubbles at shallower water depth might not contain CO_2 anymore, such bubbles still serve as a proxy for gas leakage at larger depth potentially releasing CO_2.

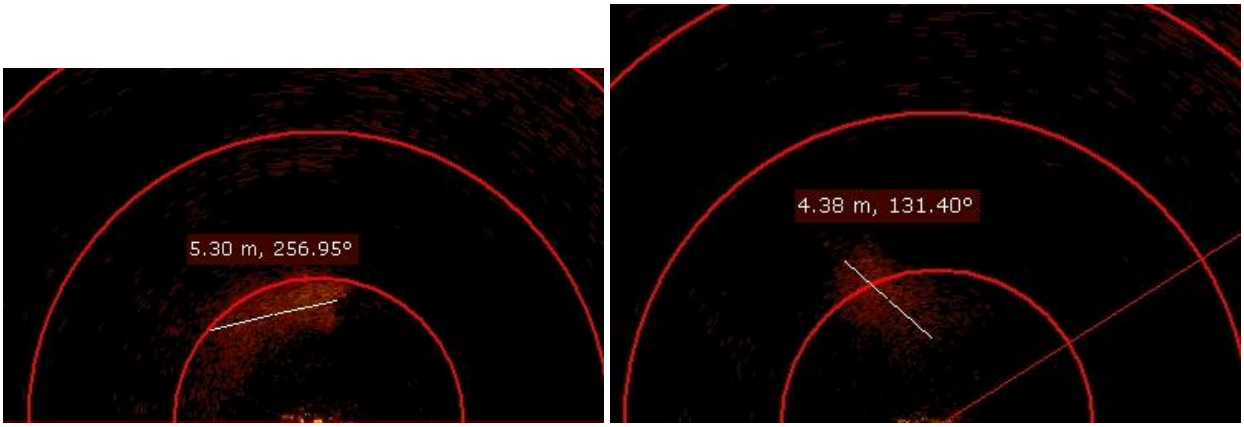

Fig. 10: Acoustic images gathered with the ROV mounted KONGSBERG MS 1000 with 200 kHz showing the bubble plume at (a) 47 m and (b) 16 m water depth with respective plume across dimension. Semi-circle distance is 3 m.

Bubble Box observations

To quantitatively assess gas fluxes and to qualitatively investigate bubble rise behavior the B-Box was developed and deployed at four dives at various gas seepage sites. The images grabbed from B-Box video recording show good quality with hardly any motion blur of the bubbles. Discrete gas flux measurements revealed fluxes around 330ml per minute at 60m depth and serve as a base to cross-check later video bubble size analyses. Considering the known ground base dimension of the bubble box frame of 0.2 m^2 and a measured integrated flux after computational “bubble trajectory” will allow for true flux assessments. By near range sonar measurements (Fig. 10) this flux will be spatially extrapolated to obtain a total flux value for one entire seep. To constrain potential bubble plume and upwelling effects a dye was injected at the base of the B-box (Fig. 11). First analyses of the videos indicate significant upwelling of the water surrounding the gas bubbles. Further evaluation of the data will finally allow to quantitatively assess gas bubble sizes, rise velocities, seep characteristica and finally fluxes.

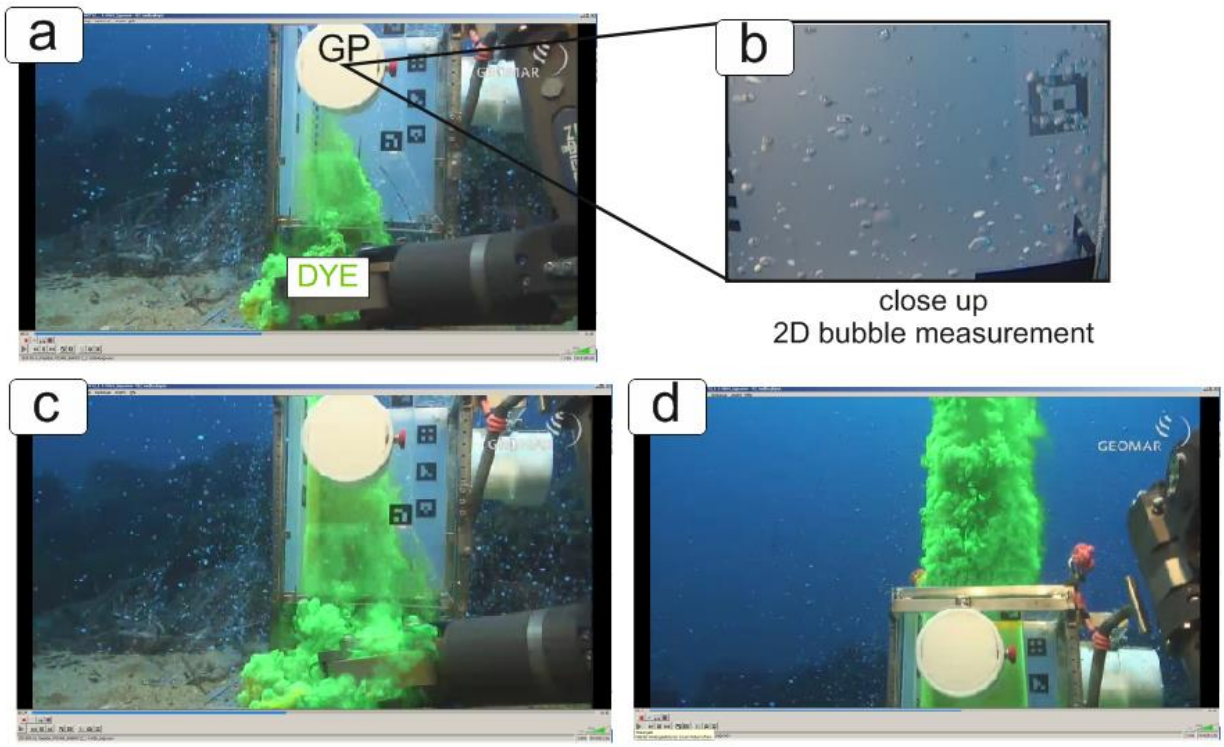

Fig. 11: Deployment of B-box at 60 m water depth showing (a) ROV camera observation of initial dye release (b) pictures taken by the GoPro (GP) with backlid illuminated gas bubbles within the bubble box. Squares in lower left corner are 1 cm, large squares on the right 4 cm. (c) ROV camera observation of tracer experiment shortly after (a) and a few seconds later (d) showing the vertical evolution of a gas bubble plume.

Highlights

- Crater shaped seabed depressions found at 70m (shaped by past eruption?)
- First online beam stack history of multibeam echosounder data allowing quick online seepage detection and CTD monitoring
- Some of the CO_2 bubbles released at 70 m depth do rise up the seasurface with. As such "high rising " features clearly emerge in remote acoustic surveying as a distinct data pattern, we acertain WCI as a very powerful seepage detection feasibility even for soluble CO_2 seepage
- Successful plume process assessment performed with B-Box and ROV sonar

4.2 Water/gas sampling and hydrographic monitoring

Mark Schmidt, Stefan Sommer, Peter Linke, Sergiy Cherednichenko

Introduction

Natural discharge of CO_2 from the seafloor is a common phenomenon and is related to a variety of different geological settings such as hydrothermal venting and submarine volcanic exhalations (e.g. Lupton et al., 2006; Italiano & Nuccio, 1991), or migrated fluids from deep sedimentary strata (e.g. McGinnis et al., 2011a). The "Panarea gas vents" represent one of the world's natural areas, where carbon dioxide is the main (>90%) gas component naturally emitted from the seafloor into the water column (e.g. Kirk, 2011, and literature cited therein). Numerous venting areas off Panarea showing different strengths of gas discharge have been located in shallow waters (~10m) in the past and recently in deeper (40-100m) areas (e.g. Monecke et al., 2012, McGinnis et al., 2011b). To test new monitoring

techniques and strategies developed for detection and quantification of CO_2 seepages from the seafloor advanced chemical/oceanographic sampling was conducted during this cruise POS469.

Sampling areas

Panarea

During cruise POS469 4 hydrocast stations and 7 pump-CTD tracks were performed in the area off Panarea (Fig. A). Water column chemistry in areas of gas (bubble) seepage where investigated in detail at seepage sites (areas Pump-CTD 3-7) which show different strengths of gas bubbling.

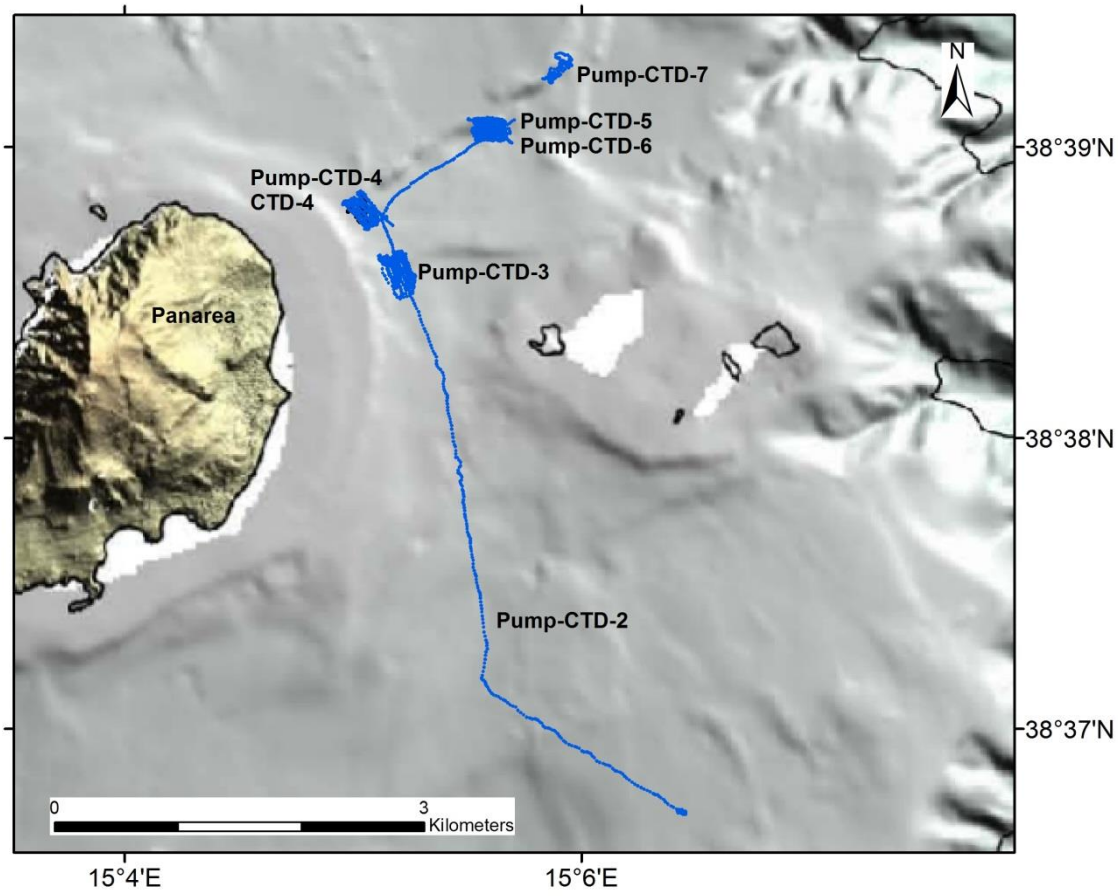

Fig. 12: Bathymetric map of Panarea (Chiocci et al., 2013) with marked (blue lines) CTD tracks (for sampling stations see table 3).

Transit

Additionally, one long transit track from Panarea (Italy) to Malaga (Spain) was used to measure (sub)surface water parameters of the Mediterranean Sea (Fig. 4).

Methodology

"Multi-purpose" rosette

The newly designed Water Sampler Rosette system (Fig. 13) was used to study the carbonate inventory (e.g. DIC, TA, pCO_2, pH) at selected water depths between 5 to 100 m in the Panarea area. The system

was towed by winch 2 from the board site of RV Poseidon and water depths were controlled by pressure readings or direct video observations near the seafloor. The digital video and data telemetry system (Linke et al., subm.) providing real-time monitoring of the seafloor was used to control the distance to the seafloor in “bottom view” mode. A HD-video camera and light sources were attached to the lower part of the frame and controlled by external telemetry (Sea and Sun Technology GmbH, Trappenkamp) via the coaxial cable. Moreover, an in situ multi-phase pump was attached to the winch cable connecting an on board Membrane Inlet Mass Spectrometer and an on board Total Alkalinity titrator with the rosette by a 1 inch plastic tube (Fig. 13).

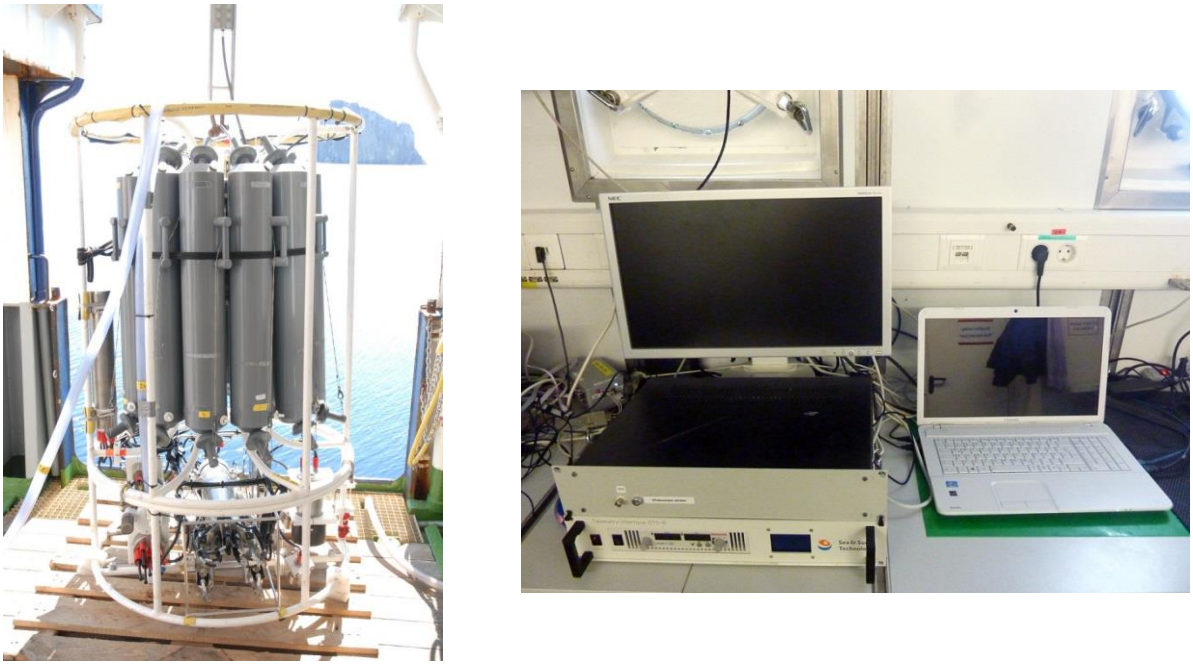

Fig. 13: Water Sampler (12 x 10-L Niskin) Rosette including SBE9plus CTD, pH sensor (SBE27), and HydroC^{TM}-CO_2 sensor with external powerpack (lower frame-left); the inlet of the plastic tube is located in the lower frame near the membrane inlet of the HydroC-CO_2 sensor. Right: Telemetry deck unit with power supply, GPS unit, labtop and external screen for full control of video, lights, CTD data transmission and bottle firing.

SBE9plus CTD

The SBE 9plus underwater unit was equipped with 2 pressure sensors, 2 temperature sensors, 2 oxygen sensors and 2 conductivity sensors. The underwater unit was controlled via the winch’s coaxial-cable by using a newly developed modem/power unit from SST (Linke et al., subm). CTD data monitoring and recording was performed with SEASAVE software (version 4.21). CTD data were recorded with 24 Hz. GPS position data was logged parallel to the CTD and Video data from an external GPS device mounted near the CTD winch.

4 analogue channels at the SBE underwater unit were used for external sensor reading (pH-, ORP-, HydroC-CO_2-, Fluorescence-sensor). The distance between CTD and the seafloor was controlled by video observation.

Hydrocasts and hydrographic data from towed CTDs were processed by using SBE software SBE7.23.1. Usually data files of 1 minute bins and 1 meter bins were created from raw data files and exported to ASCII. CTD data will be combined with data sets derived from Membrane Inlet Mass Spectrometry (MIMS), online TA-titrations, and HydroC-CO_2 measurements. All data sets are correlated with their UTC time stamps.

SBE27-pH/O.R.P. sensor

The sensor (SBE27-0202) combines a pressure balanced glass-electrode, Ag/AgCl reference probe, and a platinum O.R.P. electrode (1200 m rated). The recent calibration equation provided by Seabird (18.03.2014) is used for the Seasave output data files.

HydroC^{TM}-CO_2 sensors

The HydroC-CO_2 (0412-006) sensor, equipped with pumped (Seabird) sensor head, was integrated into the video-CTD device. Technical specifications of the sensor are given in table 2. The measured data is stored internally on SD card, however, the sensors reading is also monitored onboard by using one analogue 0-5V channel of the SBE9plus.The HydroC^{TM}-CO2 is powered by an external NiMH-power unit (>10h at ~16°C).

Table 2: HydroC-CO_2 sensor specifications.

	HydroC^{TM}-CO_2
Measuring range	100-6000 ppm
Resolution	1 ppm
Response time (t63)	1 min
Warm-up time	~10 min
Operational depth	2000

Dissolved gas and DIC sampling

For determining Total Alkalinity (TA) and Dissolved Inorganic Carbon (DIC) content of seawater in the working area by using conventional titration methods (Dickson et al., 2007), Niskin water samplers were fired at selected depths and locations during CTD tracks and casts (Water depths between 5 and 100 mbsl). Video observation, pH, and pCO_2 data were used for selection. After CTD recovery, seawater samples were transferred from Niskin bottles to 500 ml Schott glass bottles. The bottles were closed, after adding 100 µl saturated $HgCl_2$-solution, with a greased glass stopper leaving a head space of about 3-5 ml. The DIC and alkalinity determinations will be conducted at GEOMAR. The pCO_2 calculations will be performed according to Lewis and Wallace (1998). Calculated pCO_2 values will then be compared with calibrated HydroC-CO_2 sensor data, and MIMS pCO_2 data.

Thermosalinograph

Underway temperature and salinity data were recorded during cruise POS469 by using the shipboard thermosalinograph. Sub-surface waters were pumped from a port well at about 4 m water depth (inlet temperature is measured by SBE38), through a shipboard tubing system, where temperature and conductivity is continuously measured with a SBE21 probe. The water is then provided for additional measurements within a tank (e.g. recording Sound Velocity) or at water taps in the laboratories (e.g. for underway Total Alkalinity titration).

Bubble sampling

A gas-tight bubble sampler (stainless steel; funnel inlet; Fig. 14) had been designed for free gas sampling at in situ pressure (max. 160 bar). The sampler was operated by ROV Phoca for capturing gas bubbles emanating from the seafloor. The gas bubble flux was calculated by monitoring the gas overflow from the sampler into the plastic funnel (Fig. 14). The inlet valve of the sampler was closed at the seafloor after the volume was totally filled with gas. Onboard sub-sampling of the high-pressure bubble sampler was conducted in a vacuum system (Fig. 15), which allowed pressure controlled release of gas into head space glass vials (up to 1,05 bar).

Fig. 14: High-pressure Bubble Sampler with funnel inlet.

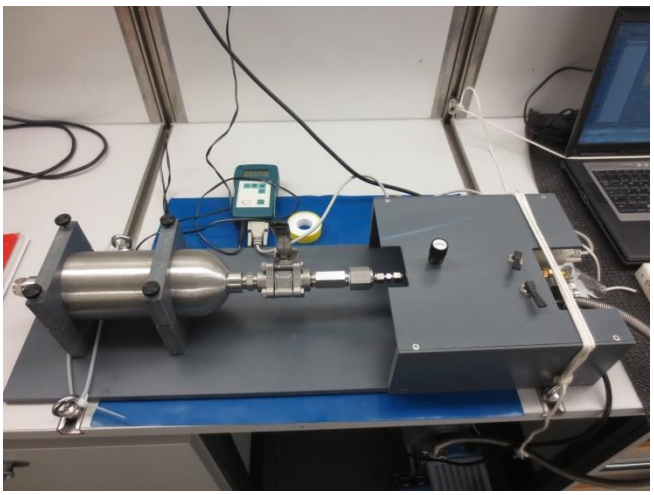

Fig. 15: Vacuum sub-sampling system for transferring high-pressure gas into head space vials.

Onboard gas chromatography

Head space gas samples derived from ROV sampling campaigns and shallow water dives where analysed for their CO_2, CH_4 and nitrogen + oxygen content by onboard gas chromatography (Fig. 16). The Shimadzu 2014 was equipped with TCD and FID (carrier gas: He 5.0; on-column injection; Porapak Q 80/100 ; FID gases produced by H_2- and air-generators).

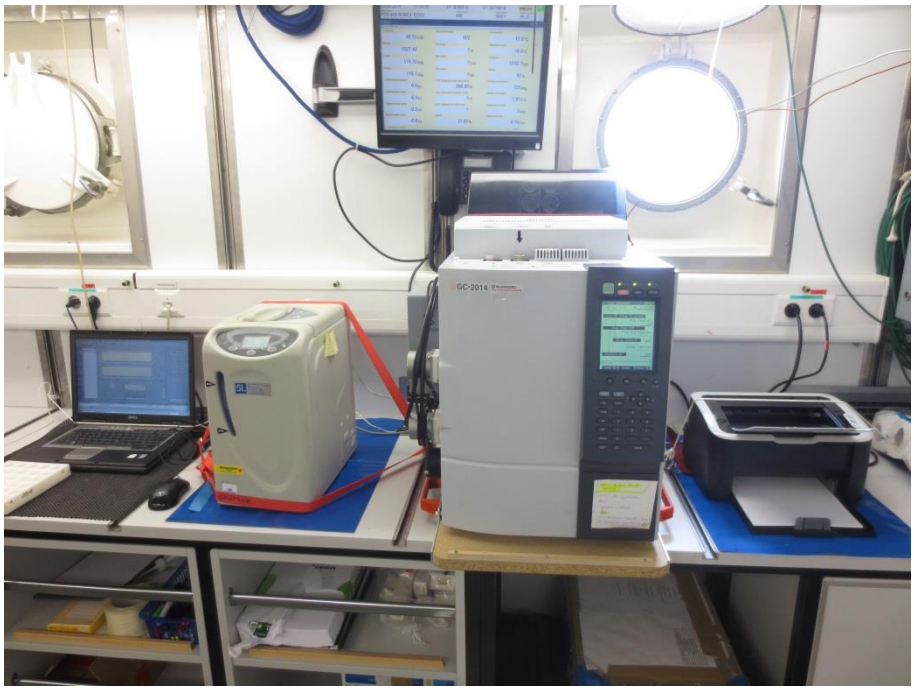

Fig. 16: Onboard gas chromatography for analysing CO_2, CH_4, N_2/O_2.

Preliminary results

About 2-7 hours long towed CTD tracks were successfully conducted in CO_2-seepage areas off Panarea (Fig. A). The area coverages above seep sites were about 200 x 400 m each at selected water depths. Selected monitoring depths of the towed Pump-CTDs were in most cases about 1 m, 5 m, and 10 m above seafloor. Parallel to the in situ CTD, HydroC-CO_2, and pH data recorded during seven Pump-CTD stations, onboard gas measurements by using Membrane Inlet Mass spectrometry and Total Alkalinity titrations were successfully conducted with waters pumped up from depth (see respective MIMS and TA chapters).

One 7 km long search profile (Pump-CTD-2) was conducted at the beginning of the sampling campaign only in bottom view mode (1-2 m above seafloor). CTD data, GPS position data, pH, HydroC-CO_2 (analogue output) data are summarized for reference samples taken for onshore DIC and TA measurements in table 3.

Station CTD4 was conducted to run 9 vertical hydrocasts within the CO_2-seepage area of Pump-CTD4 (Fig. 12). Additional CTD hydrocasts (CTD1-3 in Tab. 3) were conducted to determine oceanographic data in the water column of the working area off Panarea.

Onboard gas chromatographic results show that ROV-sampled gas bubbles contain more than ~95% CO_2 (Tab. 4). Methane is in the range of several thousand ppmV and air (probably mainly N_2/O_2) is <3%. H_2S was not determined onboard.

The onboard gas gromatographic analysis also helped to improve the sampling strategy of shallow gas vent sampling performed by the land-based diving group (see chapter 4.6). Gas samples captured from 0-1.2 m above seafloor contain >93%Vol. CO_2, and CO_2-concentrations in gas bubbles decrease with increasing distance to seafloor (i.e. down to 20%Vol. at 12 m above seafloor).

Tab. 3: Summary of oceanographic data measured when Niskin bottles were fired during Pump-CTDs (PCTD) and vertical CTD casts (CTD).

Station	*Bottle*	*Date*	*Water Depth (m)*	*Latitude (°N)*	*Longitude (°E)*	*Temperature (°C)*	*Oxygen (mL/L)*	*Salinity (‰)*	*pH*	*Sound Velocity (m/s)*	*pCO2 (µatm – analogue output)*
PCTD1 Stat. 572	1	May 05 2014 07:14:21	37.6	38.62222	15.09306	15.920	5.33	37.756	8.14	1515	357
PCTD2 Stat. 577	1	May 06 2014 13:51:01	47.7	38.6417	15.0875	15.364	5.39	37.831	8.01	1512	522
	2	May 06 2014 14:00:13	47.7	38.64298	15.08678	15.345	5.39	37.834	7.87	1512	745
PCTD4 Stat. 588	1	May 09 2014 11:17:43	44.1	38.64584	15.08444	15.572	5.44	37.776	7.86	1513	630
	2	May 09 2014 11:20:15	44.7	38.64608	15.08416	15.545	5.41	37.776	7.79	1513	827
PCTD5 Stat. 591	1	May 10 2014	75.2	38.651	15.09344	14.799	5.26	37.922	7.51	1511	1503

		15:21:37									
	2	May 10 2014	75.4	38.65098	15.09346	14.771	5.25	37.930	7.89	1511	1992
		16:17:35									
PCTD7 Stat. 602	1	May 13 2014	72.7	38.65433	15.09768	14.735	5.15	37.959	6.98	1514	3792
		12:56:26									
	2	May 13 2014	71.3	38.65424	15.09758	14.795	5.23	37.925	7.47	1514	4816
		12:58:08									
CTD1 Stat. 569	1	May 04 2014	83.7	38.619	15.09652	14.638	5.15	37.950	8.13	1510	355
		06:30:41									
	2	May 04 2014	79.2	38.61902	15.09652	14.705	5.26	37.902	8.14	1510	355
		06:31:22									
	3	May 04 2014	74.3	38.61904	15.09646	14.718	5.29	37.897	8.15	1510	342
		06:32:25									
	4	May 04 2014	67.6	38.61904	15.09642	14.935	5.33	37.845	8.11	1510	363
		06:33:56									
	5	May 04 2014	65.5	38.61906	15.09648	14.938	5.32	37.844	8.10	1510	384

		06:35:35									
	6	May 04 2014	65.5	38.61906	15.0965	14.938	5.31	37.844	8.11	1510	384
		06:36:11									
	7	May 04 2014	63.6	38.61908	15.09656	14.936	5.33	37.844	8.12	1510	380
		06:37:34									
	8	May 04 2014	58.5	38.61905	15.09652	15.030	5.37	37.812	8.15	1510	369
		06:38:52									
	9	May 04 2014	48.7	38.61902	15.09654	15.366	5.40	37.753	8.16	1510	350
		06:39:57									
	10	May 04 2014	28.8	38.619	15.09656	16.704	5.23	37.654	8.15	1510	347
		06:42:52									
	11	May 04 2014	15.4	38.61904	15.0966	16.705	5.24	37.637	8.16	1510	352
		06:44:06									
	12	May 04 2014	5.4	38.61906	15.09662	16.752	5.24	37.623	8.16	1510	349
		06:45:35									
CTD2 Stat. 598	1	May 12 2014	69.0	38.6515	15.09282	14.776	5.25	37.936	7.49	1514	1051
		15:35:02									

	2	May 12 2014 15:35:33	63.7	38.65148	15.09284	14.967	5.36	37.865	7.59	1514	1260
	3	May 12 2014 15:35:50	58.5	38.65144	15.09286	15.081	5.38	37.833	7.83	1514	1133
	4	May 12 2014 15:36:08	53.4	38.65142	15.09288	15.160	5.39	37.815	7.91	1514	1031
	5	May 12 2014 15:36:25	48.1	38.6514	15.09288	15.253	5.39	37.803	7.99	1514	902
	6	May 12 2014 15:36:40	43.7	38.65136	15.09288	15.579	5.39	37.769	8.04	1514	820
	7	May 12 2014 15:36:56	39.4	38.65134	15.09288	15.801	5.38	37.753	8.07	1514	740
	8	May 12 2014 15:37:16	33.8	38.65134	15.09286	16.500	5.33	37.719	8.08	1514	663
	9	May 12 2014 15:37:32	28.7	38.65134	15.09284	16.828	5.30	37.713	8.11	1514	613
	10	May 12 2014	23.5	38.65132	15.09284	16.930	5.28	37.715	8.13	1514	569

		15:37:50									
	11	May 12 2014	19.3	38.6513	15.09284	16.926	5.29	37.705	8.13	1514	533
		15:38:06									
	12	May 12 2014	13.8	38.6513	15.09284	17.517	5.24	37.720	8.13	1514	496
		15:38:30									
CTD3 Stat. 599	1	May 12 2014	68.1	38.65062	15.09298	14.795	5.26	37.931	7.54	1513	794
		17:56:12									
	2	May 12 2014	68.1	38.6506	15.09296	14.798	5.26	37.928	7.51	1513	954
		17:56:23									

Tab. 4: List of measured gas samples (by onboard gas chromatography).

Station	*Device*	*Niskin Bottle (No)*	*Bubble sampler (No)*	*Glass Vial (m above seafloor)*	*Date*	*CO2 (%Vol)*	*Start*	*End*	*Longitude (°E)*	*Latitude (°N)*	*Water depth*
579	ROV2		GT1		07.05.2014	99.4	08:24:52	08:33:54	15,0863809	38.643037	43.5
580	ROV3		GT2		07.05.2014	99.6	12:11:59	12:18:34	15.0839204	38.646015	41.7
590	ROV6		GT3		10.05.2014	94.5	8:20:48	09:01:57	15.0839411	38.645873	41.1
593	ROV7	1. 2. 3	GT4		11.05.2014	98.6	08:10:35	08:12:54	15.0939987	38.651011	no data
594	Zodiac		GT5		12.05.2014	66.9			Shallow vents		0.5
601	ROV9	1. 2. 3			13.05.2014	n.a.	10:22:18	10:23:51	15.0979429	38.654854	70
602	PCTD7	1. 2			13.05.2014	n.a.	12:56:26	12:58:08	15.0976	38.6543	71-73
PAN3-STA5	Diver			0. 0.4. 0.8. 1.2. 1.6		95-93			Shallow vents		
PAN3-STA8	Diver			0. 1. 2. 3. 4. 5. 6. 7. 8. 9. 10. 11. 12		96-20			Shallow vents		

4.3 Membrane Inlet Mass Spectrometry (MIMS)

Stefan Sommer, Sergiy Cherednichenko

Methodology

Similar to the approach of Mächler et al. (2012) and Sommer et al. (subm.), an underwater pump, typically used for rural sewage treatment, generated a continuous water stream through a 60 m long hose (i.d.: 2.5 cm) from the CTD to the laboratory at a rate of 37.5 l min^{-1}, were quasi continuous inline Membrane Inlet Mass Spectroscopy (MIMS) gas measurements were made ex situ. The inlet of the hose was mounted on the CTD frame close to the CONTROS sensor (Fig. 13), whereas the pump was clamped onto the CTD wire at a water depth of about 25 to 0 m. Parts of the hose, which were exposed to sunlight on deck were thermally insulated by wrapping it into rescue cover sheets. Subsampling of water from this hose took place in the laboratory by using a steel capillary (i.d. 1.1 mm) that was connected to a glass membrane inlet. The distance between the location of subsampling and the membrane inlet was about 150 cm (Fig. 17).

Fig. 17: Onboard setup of the MIMS in the wetlab of RV Poseidon.

To allow best possible temperature stability of the membrane inlet it was kept submersed in a water bath using a Dewar vessel whose temperature was controlled using a water bath (Julabo F34). During deployments the temperature of the inlet increased by a maximum of 0.2°C. Constant flow of the subsampled water through the membrane inlet was achieved using a peristaltic pump (Ismatec) at a flow rate of 2.5 ml min^{-1}. Within the glass inlet the water was sucked through a permeable silicone tube (Dow Corning, Cat.No. 508-007, length 40 mm, i.d. 1.57 mm). Gas flow from the inlet to the quadrupole mass spectrometer was supported with Helium that was supplied through a fused silica capillary (i.d. 100 µm). An inline cryo-trap (– 35° C, ethanol) between the inlet and the mass spectrometer was used to reduce water vapour. The CO_2 concentration (pCO_2) of the dry gas stream was then determined by using a Prisma Plus™ quadrupole mass analyser (1-100 amu, channeltron SEM, closed ion source) pumped by HiPace80 turbo molecular pump (Pfeiffer) and RC6 hybrid pump (Vacuubrand). Partial pressures of CO_2 were calculated from calibrated ion currents at the mass to charge ratio of 44. Ion currents of pCO_2 were calibrated using pCO_2 standards of 300, 1000, 5000, 10000 ppm. These standards were produced by equilibrating pre-filtered (0.2 µm) seawater with respective standard gases at the in situ temperature for 30 min in a water bath (Julabo F34).

Laboratory tests confirmed that the time period of 30 min is sufficient to reach equilibrium for methane, which has a lower solubility than CO_2 (Walther, 2013).

Data evaluation

The sampling interval of the MIMS was 1.45 s but readings were binned into a 20 s interval, which at a towing speed of 0.3 knots resulted in a spatial resolution of 3 m. During post-processing the sampling time of the MIMS data was coordinated with the sampling time of the CTD system which concurrently to the physical data further received the NMEA position signal of an external GPS allowing for geo-referencing of the pCO_2 data. The time period between water sampling at the inlet of the CTD and its arrival at the membrane inlet in the laboratory was about 2 min but is not back-calculated in the averaged data set of PCTD3. Moderate gas bubbling has been observed here during ROV and Video-CTD operations at the seafloor and this combined data set has been analysed and results prepared for publication (Schmidt et al., subm.).

4.4 TA Measurements by means of a new FIA System

Steffen Aßmann, Peter Linke, Nadja Kinski

Objectives

At CO_2 release sites the marine carbonate system – as the dominating buffer system in seawater – is strongly affected by the natural gas emissions. High CO_2 concentrations shift the chemical equilibrium of the CO_2 system due to the dissolving CO_2, which acts as an acid in water. For understanding the fate of released CO_2 it is necessary to determine comprehensively the carbonate system parameters at a high spatial and temporal resolution. Therefore total alkalinity (TA) and the partial pressure of CO_2 (pCO_2) are measured continuously using both, a pumped CTD for deep water body and an underway setup for surface water measurements.

Often TA is estimated from salinity since these parameters are closely related. This is convenient for open ocean scenarios, but not for dynamic coastal areas with many processes that potentially change TA. The combination of TA and pCO_2 allows for a full characterization of the carbonate system. In addition this parameter combination is favored as it results in comparatively low errors for the calculated values based on an advantageous error propagation. In contrast the often used combination pH and pCO_2 results in high errors when calculating the missing parameters.

Methodology

Measurement Principle

The newly developed autonomous TA-System (HydroFIA™ TA, CONTROS GmbH) applies an acidic titration on a seawater sample of defined volume. For the subsequent pH determination absorbance measurements of an acid-base indicator dye Bromocresol green are carried out. Due to the open-cell titration (i.e. the formed CO_2 is completely removed from the sample) only one titration point is needed for measuring TA.

Underway measurements

During transit time the TA-System was set up in the wet laboratory together with a pCO_2 sensor (HydroC™ CO_2, CONTROS GmbH) for continuous measurements of the surface water (Fig. 18). The TA-System was fed using a bypass with approx. 20 L min^{-1} ending in a flow through box containing the pCO_2 sensor. For the characterization of the carbonate chemistry the CTD data provided by the ship are used.

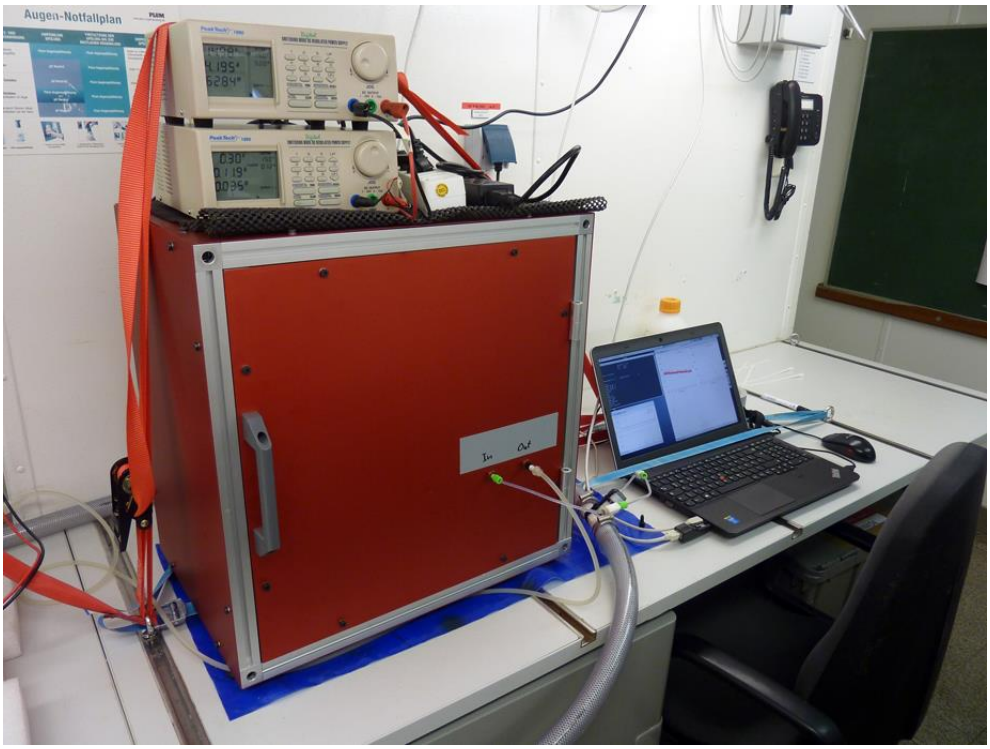

Fig. 18: Set up the autonomous TA-System in the wetlab of RV Poseidon.

Pump CTD

For mapping the natural CO_2 seep sites a CTD was used together with an underwater-pump transporting the deep water to the wet laboratory of the ship. During deployment the pump was kept at constant depth. The seawater was continuously measured in the lab. Other parameters such as salinity, temperature, pH, pCO_2 were measured under water directly at the CTD.

Discrete Samples

Discrete water samples were taken for quality assurance of the measured data. DIC and TA of these samples will be measured in the laboratory at GEOMAR to serve as reference values. Furthermore, samples have been taken during up- and down-casts of the CTD for a vertical TA profile of the water column in the survey area (data not shown).

Preliminary Results

The newly developed TA-System has been successfully used for the first time on a research vessel. The measurements were stable and reproducible. In the examined area the strong variation of the CO_2 concentrations were not affecting the TA values due to its insensitivity against variations in pCO_2, providing a stable parameter during these highly dynamic conditions.

Figure 19 shows continuous TA and salinity data measured during the transit from Panarea to Malaga documenting the steadiness of the system. A total of 1437 measurements were collected at a measuring interval of 5 min. The gap at 18th May is due to maintenance work of the system. The system consumes acid and indicator, which needed replacement after approx. 1600 measurements.

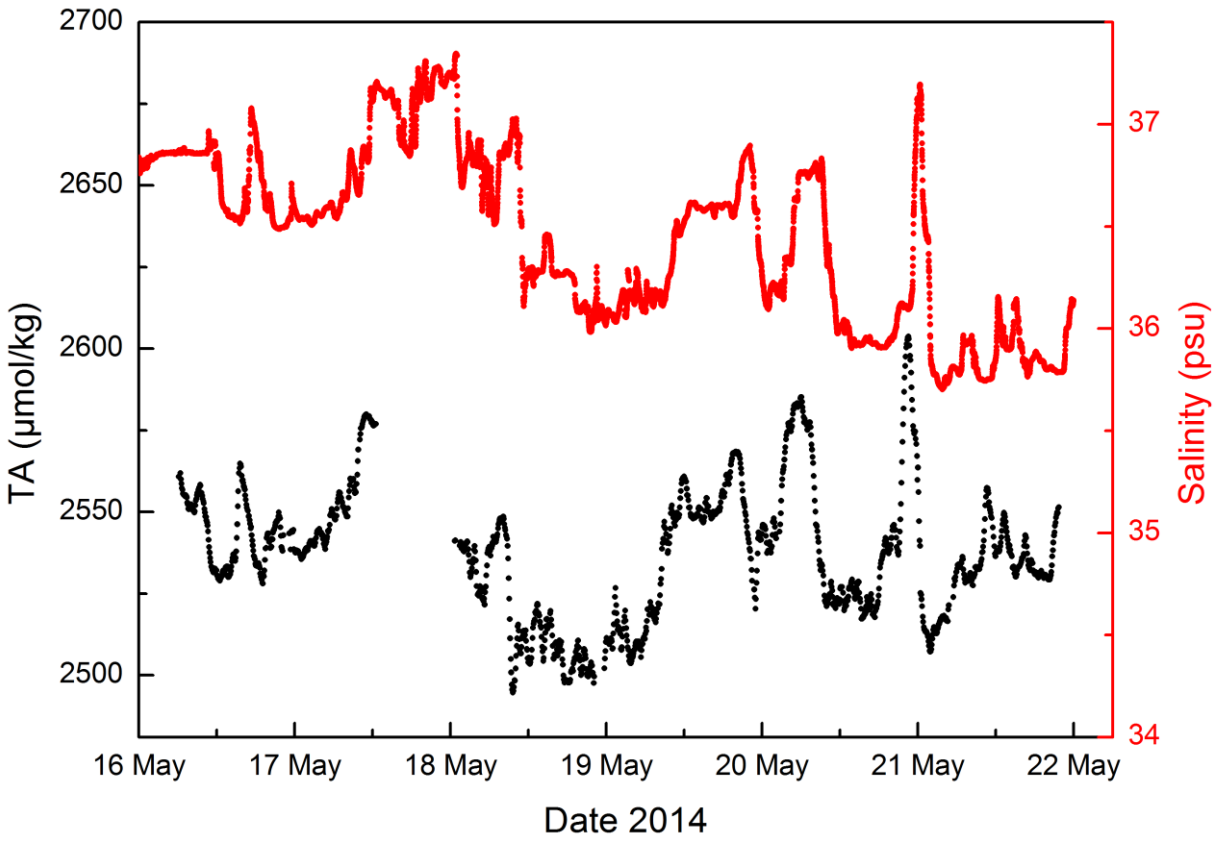

Fig. 19: Preliminary continuous TA and salinity data measured during the transit from Panarea to Malaga.

Reference samples have been taken and certified reference materials (CRM) have been measured regularly during the cruise. Final evaluation of the data will give more information about the accuracy of the system. An overall precision of the measured data was found to be less than ±3 µmol kg^{-1}. This value was found for continuous sample measurements during the transit from Panarea to Malaga. Therefore, the standard deviation of at least 10 values has been taken several times at gradient free areas of the measured data.

4.5 ROV deployments

Peter Linke, Martin Pieper, Matthias Bodendorfer, Patrik Cuno, Jan Hennke, Hannes Huusmann

ROV PHOCA is a 3000 m rated deep diving platform manufactured by SubAtlantic FET, Aberdeen, Scotland. It is based on commercially available ROVs, but customized to our demands, e.g. being truly mobile. ROV PHOCA has previously been operated from the medium sized German research vessels POSEIDON and ALKOR. As an electric work class ROV of the type Comanche, this is build No. 21. ROV PHOCA is based at GEOMAR, the Helmholtz Centre for Marine Sciences Kiel, Germany.

For shallow-water applications, a 28 mm Aramid mantled cable (neutrally buoyant tether, 500m) is used, which is paid in and out manually, using a capstan winch (Fig. 20) mounted on the deck. For underwater navigation, a mobile ORE system was used with an autonomous transponder mounted on the light rack of the ROV and the transducer mounted on a pole on the starboard site of the vessel. The 20'-control container was placed next to the fishing winch on the portside container place. ROV PHOCA is equipped with a tool skid onto which a variety of tools to customers demand can be mounted (Fig. 20).

Fig. 20: ROV PHOCA with bubble box on the its porch ready for deployment on the aft deck of RV Poseidon with capstan winch for tether management in the back (top left). ADCP on the porch prepared for deployment (left). Extracted drawers with CO_2- sensor and gas sampler in the sampling box on the starboard side and 3 Niskin samplers on the portside of the ROV.

For more details on the ROV system please visit http://www.geomar /PHOCA.

A gastight gas sampler was deployed by the ROV on different occasions to collect gas samples for GC analyses. A CO_2 sensor (Contros) was mounted on the ROV and partly integrated into the ROVs telemetry system, allowing on-line readings for real time control of the sensor data. Niskin bottles mounted on the portside drawer of the ROV were used to collect samples of ambient water as well as CH_4 and CO_2 enriched bottom water (Fig. 20). More details on individual dives and respective scientific results are given in the scientific chapters of this report.

Preliminary results

The work class ROV PHOCA was used for sampling of gas and bottom water, for obtaining on-line readings of a CO_2-sensor, and for deployment and recovery of autonomous instruments (e.g. ADCPs, bubble box). During cruise POS469, 11 scientific dives (Tab. 5) were completed. Maximum diving depth was about 80 m and maximum bottom time was 4:10 hours. In total, bottom time accumulated to approx. 22 hours (total dive time 24.5 hours).

Table 5: ROV station list during cruise POS469.

Station Number POS469	Dive No.	Date	Time Start (UTC)	At Bottom (UTC)	Off Bottom (UTC)	Time End (surface) (UTC)	Location	Depth (m)	ROV Bottom Time (h)	ROV Dive Time (h)
	1	01.05.2014	Harbour Test Bari							
576ROV01	2	06.05.2014					Panarea		00:00	00:00
579ROV02	3	07.05.2014	06:59	07:11	08:40	08:48	Panarea	44	01:28	01:48
580ROV03	4	07.05.2014	10:53	11:01	14:57	15:04	Panarea	68	03:56	04:10
583ROV04	5	08.05.2014	07:17	07:19	08:11	08:16	Panarea	51	00:51	00:59
586ROV05	6	09.05.2014	07:03	07:05	09:02	09:10	Panarea	46	01:57	02:06
590ROV06	7	10.05.2014	06:48	06:55	10:12	10:19	Panarea	47	03:17	03:30
593ROV07	8	11.05.2014	07:02	07:08	09:59	10:06	Panarea	70	02:50	03:03
596ROV08	9	12.05.2014	07:06	07:13	09:38	09:44	Panarea	74	02:24	02:37
601ROV09	10	13.05.2014	07:05	07:14	10:41	10:46	Panarea	70	03:26	03:41
604ROV10	11	15.05.2014	11:50	11:55	12:09	12:16	Panarea	42	00:14	00:26
605ROV11	12	15.05.2014	13:10	13:16	13:47	13:58	Panarea	73	00:31	00:48
606ROV12	13	16.05.2014	09:07	09:13	10:17	10:25	Panarea	41	01:04	01:17
Total: 11 scientific dives									22:03:28	24:30:42

576ROV01: Unfortunately, the first ROV station had to be abandoned due to technical problems with the ship's data protocol.

579ROV02: The second ROV dive repeated the previous pump CTD survey and we discovered some small chimneys with shimmering water and we obtained a gas sample at a site with moderate gas flow and single gas outlets (Fig. 21). Just when we arrived at a larger gas venting patch we had to abandon the dive due to a ground fault alarm in the telemetry.

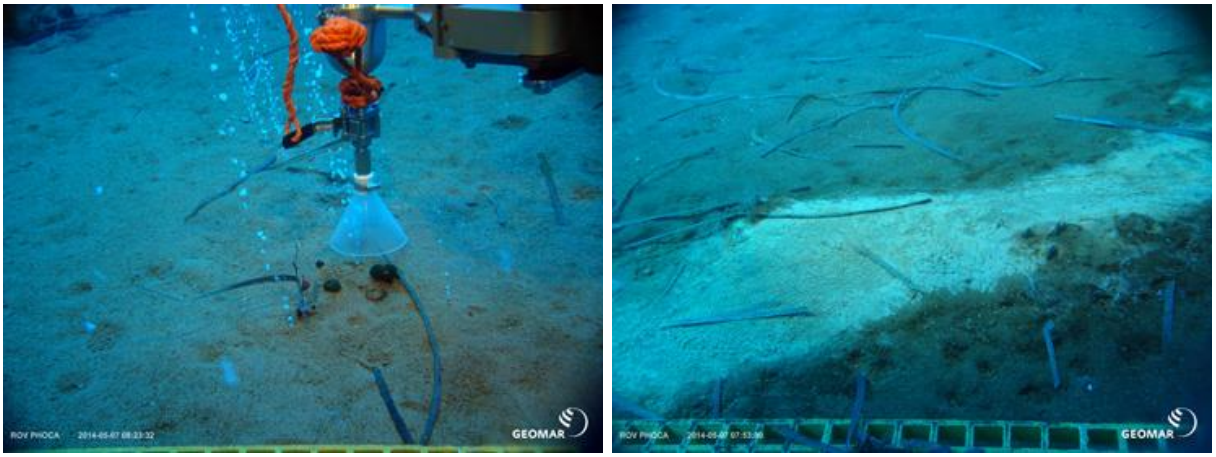

Fig. 21: View on the seafloor in the 1st gas vent field with single bubble strains sampled with the gas sampler. Furthermore, small chimneys with shimmering water and bacterial mats were found.

598ROV03: After rapid retrieval of the ROV and repair of the ground fault sensor we were able to perform a second dive at the position where the previous dive had ended (Fig. 22). During the dive we took a gas sample and 2 Niskin water samples at the gas venting patch, which was named “whirl pool”. We continued the dive along the small volcanic ridge to the east and discovered a strong gas venting activity in a crater at 70m water depth within a rough topography.

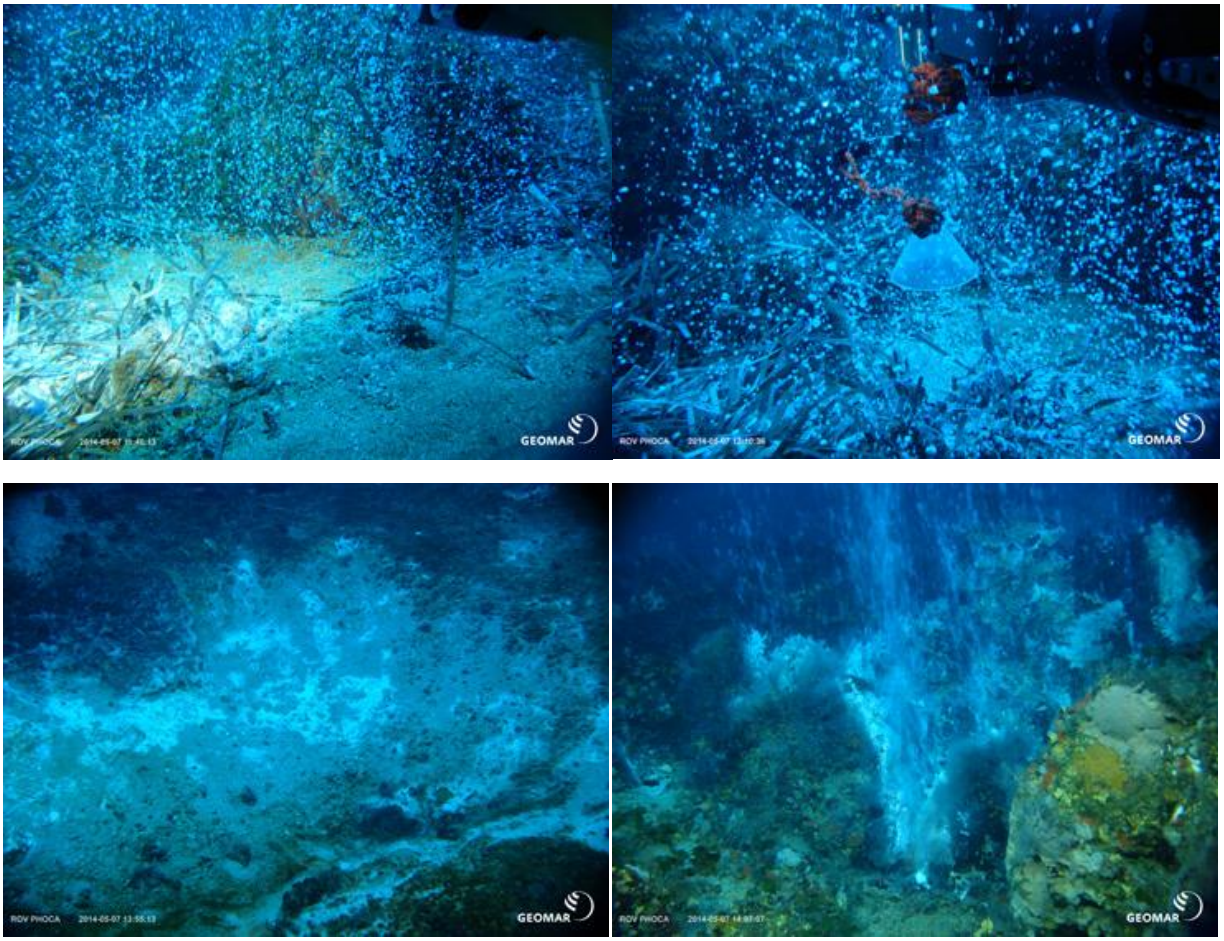

Fig. 22: (Top) the “whirl pool” site was sampled. (Below) Seafloor inside the volcanic crater covered with bacterial mats, view on the “strong vent”.

583ROV04: ROV dive 4 was very short and just to deploy an ADCP on a flat and sandy area between the 2 gas venting fields in 40 m water depth (Fig. 23).

Fig. 23: ADCP deployment by ROV.

586ROV05: During ROV dive 5 the bubble box was deployed at the 1st vent field on top of vents with single gas streams to measure the bubble sizes, rise velocity and discharge rates (Fig. 24).

590ROV06: During ROV dive 6 the bubble box was used to measure the bubble sizes and discharge rate at the whirl pool site (Fig. 24) and another gas sampler was filled for on board GC analysis.

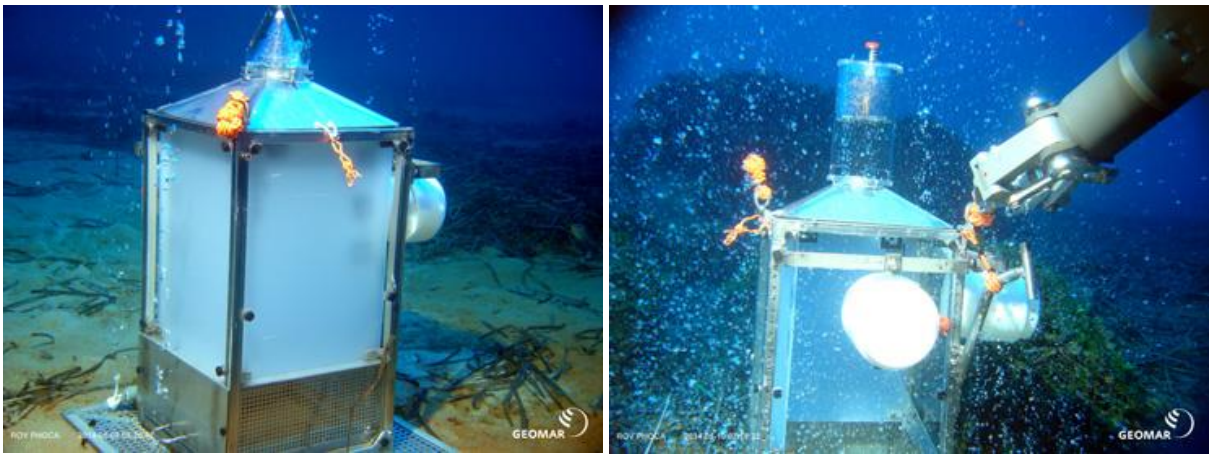

Fig. 23: Bubble box deployments at the vent field with slow discharge (left) and at the whirl pool site (right).

593ROV07: This dive was used to survey the area around the explosion crater and fill the gas sampler and 3 Niskin samples at “strong vent” (Fig. 25).

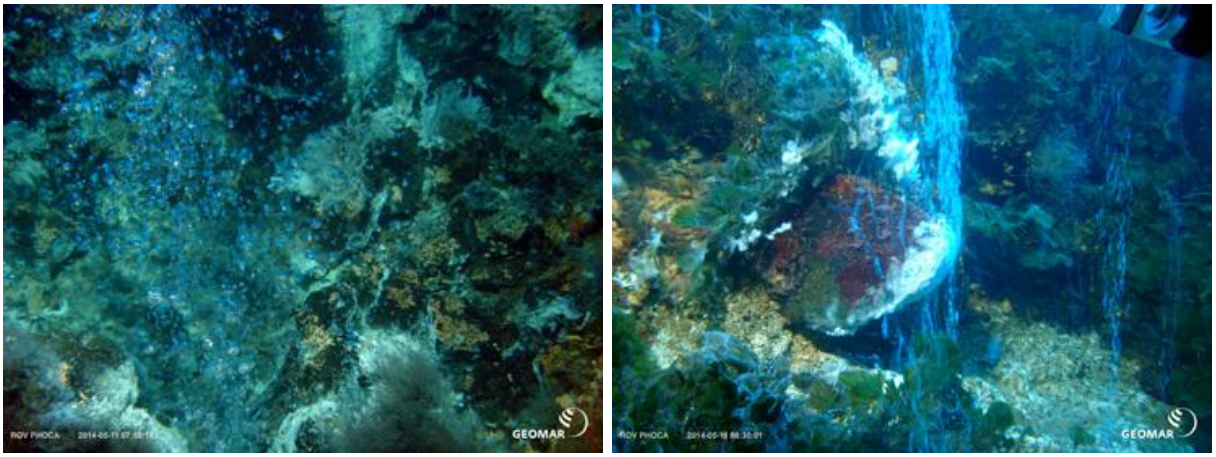

Fig. 25: Vigorous gas discharge observed at 70 m water depth.

596ROV08: During ROV dive 8 the bubble box was deployed again at the whirl pool site to conduct a stain release experiment. Furthermore, the ROV's sonar was used to trace the rising gas bubbles during their ascent through the water column.

601ROV09: During ROV dive 9, the second ADCP was deployed next to the crater with the strong vent, where later a stain release experiment and vertical sonar mapping of the rising gas bubbles was performed. After transit to a second crater we found a large lobster trap (Fig. 26) and bubbling vents in the center of the depression with the highest CO_2-concentrations of the cruise.

Fig. 26: View on the seafloor with rising gas bubbles and an abandoned lobster trap in the center of the second crater.

604ROV10 and 605ROV11: Both ADCPs were recovered during these short dives.

606ROV12: During ROV-dive 12 to the whirl pool site the bubble box measurements and the stain release experiment were repeated.

4.6 Shallow-water diving campaign

Lisa Vielstädte, Nikolaus Bigalke

Introduction and Objectives

From May 10th to May 19th the third field-campaign to a submarine CO_2-rich hydrothermal seepage site 3 km east of the Aeolian island of Panarea (Italy) was conducted in cooperation with R/V Poseidon cruise POS469. The campaign aimed (a) to study the dissolution and dispersion of natural CO_2 bubbles emitted from shallow vents using 2D- and 3D- imaging techniques as well as geochemical analyses, (b) to investigate bubble plume dynamics and (c) to measure the subsequent dispersion of the solute in the water-column. The study site "Bottaro Crater" was chosen because the shallow hydrothermal seeps constitute an ideal natural laboratory for investigating the dissolution behavior of CO_2 bubbles emitted from vents of varying strength. Results of the previous cruise ECO2-8 (2013) showed that bubbles rise faster than numerical models predict. The bubble size proved to be no sufficient indicator for their rising speed. To substantiate this observation the existing bubble parameterization rack (BPR) was improved to allow accurate imaging of bubbles during their first 2 m of ascent. In addition to optical measurements, the changing gas bubble composition during the ascent was determined. The evaluation of 3D bubble records and the geochemical data will be used to improve the parameterizations used for numerical modeling. Model applicability will be improved from low- (i.e. single bubble streams) to high leakage rates by implementing the physics of bubble plumes.

Cruise Narrative

All work at sea was conducted from an inflatable Zodiac boat hired from the Amphibia diving center. For a detailed description of the research activities please refer to the attached table of the station list (also published on www.pangea.de).

Saturday May 10th

- Arrival of L. Vielstaedte, N. Bigalke and M. Kreutzburg on the island of Panarea.

Sunday May 11th

- Arrival of C. Howe in the early morning
- Rendezvous with R/V Poseidon, discussion about study plans and retrieval of equipment
- Unpacking and assembling of equipment
- Afternoon dive:
  First overview-dive at the study site and deployment of BPR (bubble parameterization rack), CTD, and current meter (Argonaut)
- Joint dinner with colleagues from Sapienza - Università di Roma (Uni Rome), Italy and Instituto Nazionale di Oceanografia e di Geofisica Sperimentale (OGS), Italy

Monday May 12th

- Morning dive: Testing of the BPR. Rising bubbles in the back of the diffusor plate disturbed optical measurements by creating shadows on the white background.
- Afternoon dive: Repetition of the morning program with improved set-up to avoid previous problems

Thuesday May 13th

- Morning dive: Locating positions of deployed devices via GPS, re-deployment of the BPR on gravel field in the center of the crater area, where gas emission is less intense and spread out over a large area (Molari et al., 2013), gas and water sampling, 3D- and 2D- bubble imaging
- Afternoon dive:
  2D and 3D bubble imaging and gas sampling, injection of Fluorescene dye into bubble plume to visualize upwelling velocity of entrained water, vertical CTD profiling in order to determine

water-column stratification prior to heavy weather conditions predicted for the following day, recovery of sensor equipment for safety
- Handover of gas and water-samples to colleagues on board of the Poseidon for GC-analysis
- Arrival of M. Nicolai on the island, Mrs. Nicolai documents research activities

Wednesday May 14th

- Interruption of research program at Bottaro Crater due to unfavourable weather with high winds (Bft 7, moderate gale), data revision and planning of subsequent research activities

Thursday May 15th

- Morning dive:
  Vertical CTD profiling within the seepage area after wind-induced disturbance on the previous day, re-deployment of the Argonaut, video imaging of gas bubbles at Vent C to determine rise velocities, gas flow measurement at Vent C, fluorescence dye experiment at Vent C, water sampling in different heights downstream of the location of Fluorescene injection to determine solute dispersion, boat-based documentation of research activities
- Afternoon dive:
  Re-deployment of the CTD, circular injection of fluorescence dye at Vent C to visualize water entrainment at the vent base, water-sampling in different heights downstream of the dye injection

Friday May 16th

- Mrs. Nicolai boarded R/V Poseidon to continue documentation work
- Morning dive:
  Recovery of all instruments and gear due to bad weather forecast
- Packing of some of the equipment and delivery to the R/V Poseidon for the return transport to GEOMAR
- Afternoon dive:
  Gas sampling at Vent C from the seafloor to the sea surface
  Delivery of gas samples to colleagues on board of the R/V Poseidon for GC-measurements

Saturday May 17th

- Attempts to locate and sample gas vents located by colleagues from the R/V Poseidon were abandoned due to ferry traffic close by
- An alternative seepage site situated close to Panarea Island was sampled at different vertical levels, ascent of single gas bubbles rising approx. 9 m from the seafloor to the surface was imaged by video

Sunday May 18th

- Sighting and securing video material

Monday May 19th

- Departure to Milazzo by hydrofoil at 8:00 AM

Methodology

Parameterization of Gas Bubble Dissolution

Bubble Size Spectra and Bubble Rise Velocities

For the assessment of the bubble size spectrum and the bubble rise velocity the existing bubble parameterization rack (BPR) was extended in height, allowing the imaging of rising gas bubbles in the first 2 m above the seafloor (asf). Bubbles were imaged against a white polysterol plate acting as a

diffusor for a 17 000 lumen light source installed behind the plate. The back-lit illumination caused rising gas bubbles to appear as black rings on the video footage. Two tilted planes were deployed on the seafloor and positioned in front of and behind the diffuser plate to permit only bubbles directly in front of the diffuser plate to enter the field of view of the cameras. Parallel to optical measurements, physicochemical properties of the water-column were measured using a CTD SBE 37-SM MicroCAT, which was attached to one of the supporting poles of the BPR, close to the seafloor. The set-up is shown in figure 27.

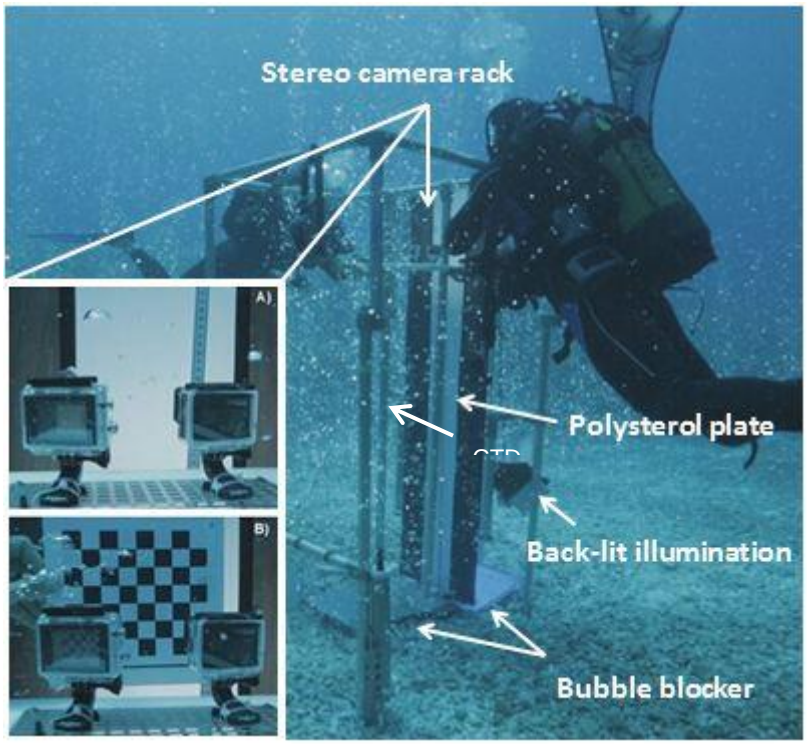

Fig. 27: Bubble Parameterization Rack for 2D- and stereo-imaging of rising gas bubbles against a white polysterol plate that acts as a light diffusor from back-lit illumination. A) Detail of the stereo-rack equipped with two GoPro cameras. B) The checkerboard is used for camera calibration to ensure the accurate determination of bubble sizes.

For 3D stereographic data evaluation of bubble sizes, two pre-calibrated action cameras (Hero III black ed. and Hero III plus black ed., GoPro Inc.) were mounted on a horizontal plate, approximately 20 cm in front of the diffuser plate (Fig. 27). The plate was vertically adjustable in 40 cm intervals. The video mode was set to VGA resolution and a framerate of 240 fps. The high framerate is crucial to allow smooth tracking of the bubbles. Additionally, bubbles were imaged in 2D using a high resolution camera (Canon 5D Mark III) to allow inter-comparison of 3D and 2D bubble images. The cameras will be post-synchronized using light signals that were applied at each measuring interval. For accurate bubble size analysis the cameras will also be post-calibrated using short checkerboard-sequences that were also recorded (Fig. 27B). The 3D reconstruction of bubbles will be based on triangulation methods.

In order to evaluate the methodological error of optical bubble size data (e.g. 2D and 3D), gas flow measurements were done in vertical intervals of 40 cm using a funnel connected to a 60 ml syringe. The volume flow derived from the bubble size spectra will be compared to the flow constrained by the funnel measurements.

Gas Bubble Composition

Gas bubbles were sampled at discrete vents of higher intensity along the crater margin as well as within the more diffuse vent of the central part of the gravel field (Molari et al., 2013) in different heights above the seafloor using 16 ml hungate tubes. A 50 ml syringe and a funnel facilitated the catching of bubbles, particularly towards shallower water-depths, where the bubble density reduces due to dissolution. In total, 47 gas samples were taken at Bottaro Crater, 21 of which from vents spread-out over the central area of the crater and in parallel to optical bubble measurements.

Additional 26 gas samples (including 13 replicates) were taken at a focused gas vent of higher intensity. Here, the hungate tubes were fixed to a vertical thread at 1 m intervals. The end of the thread was attached to a buoy at the sea surface. Gas samples were taken within the entire water-columns (Fig. 28). After sampling the hungate tubes were screwed tight at depth, which caused the vials to be slightly over-pressured after recovery. For gas analysis 100 µl sub-samples were injected into the GC to determine the CO_2, CH_4, N_2, and O_2 content. H_2S will be analyzed in the laboratory at GEOMAR.

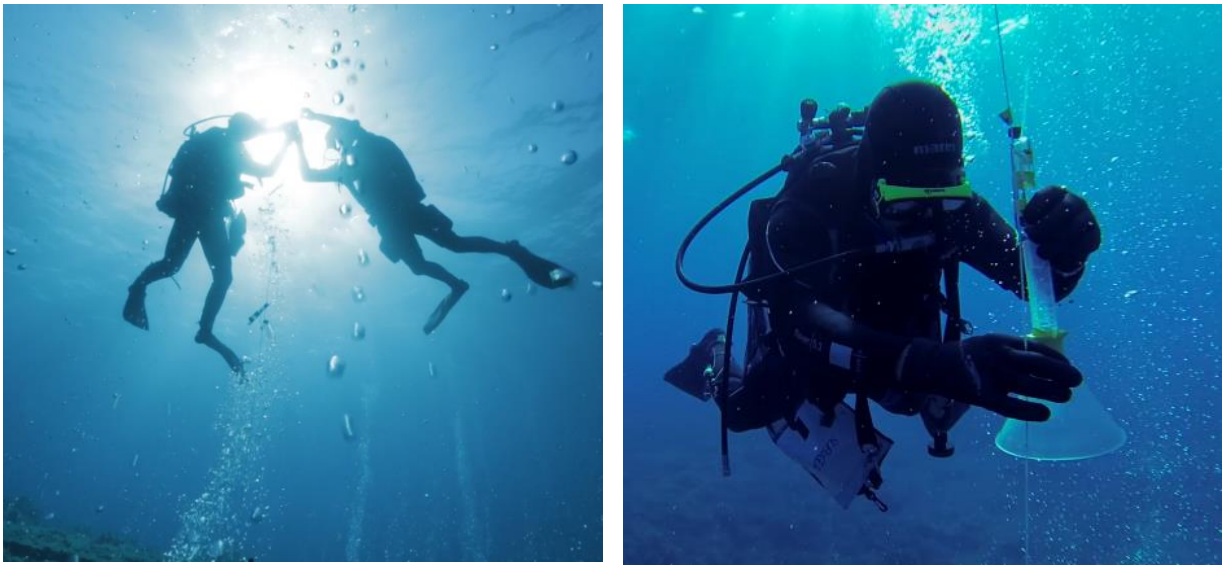

Fig. 28: Gas sampling along a vertical thread at vent C.

Water Sampling

Additionally, 42 water-samples were taken to determine the dissolved gas concentration within the ambient seawater. 100 ml headspace vials were filled with seawater in 40 cm intervals and subsequently crimped shut under-water (Fig. 29). Helium was injected into the vials in order to create a 20 ml headspace volume by partly removing the water via a compensation needle. To avoid microbial turnover effects, the headspace samples were immediately poisoned by adding 20 µL of $HgCl_2$. The headspace will be analyzed by gas chromatography at GEOMAR.

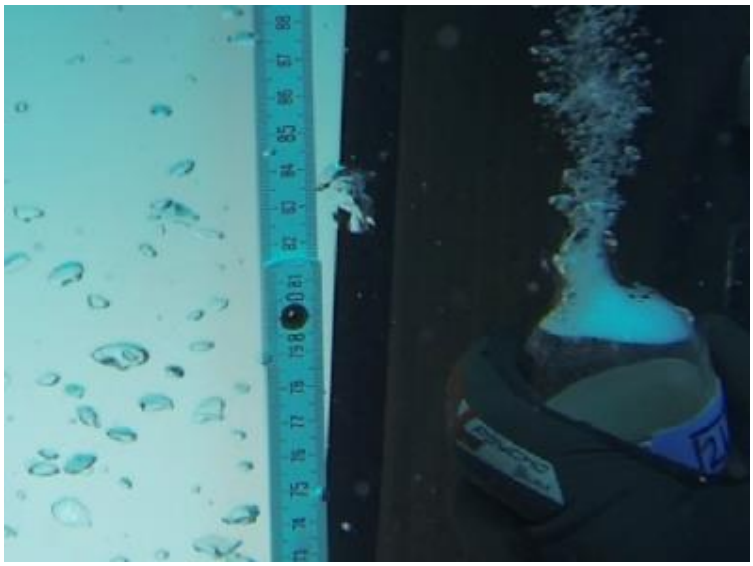

Fig. 29: Water sampling for dissolved gas analysis.

Bubble Plume Dynamics

Three fluorescene dye experiments were performed to visualize bubble plume dynamics under varying gas emissions. On the gravel field of the crater, i.e. at locally low to moderate gas fluxes, the dye was injected in parallel to BPR measurements to determine the upwelling velocity of entrained seawater from the video footage. To correlate upwelling velocity and gas emission, the gas flux was also determined by measuring the time to fill a 5 L bucket with the gas emitted at the injection site.

At the focused Vent C of higher intensity, two injection experiments were performed. In the first experiment the dye was directly injected into the vent. In the second experiment, a circular, perforated hose was arranged around the base of the vent (Fig. 30).

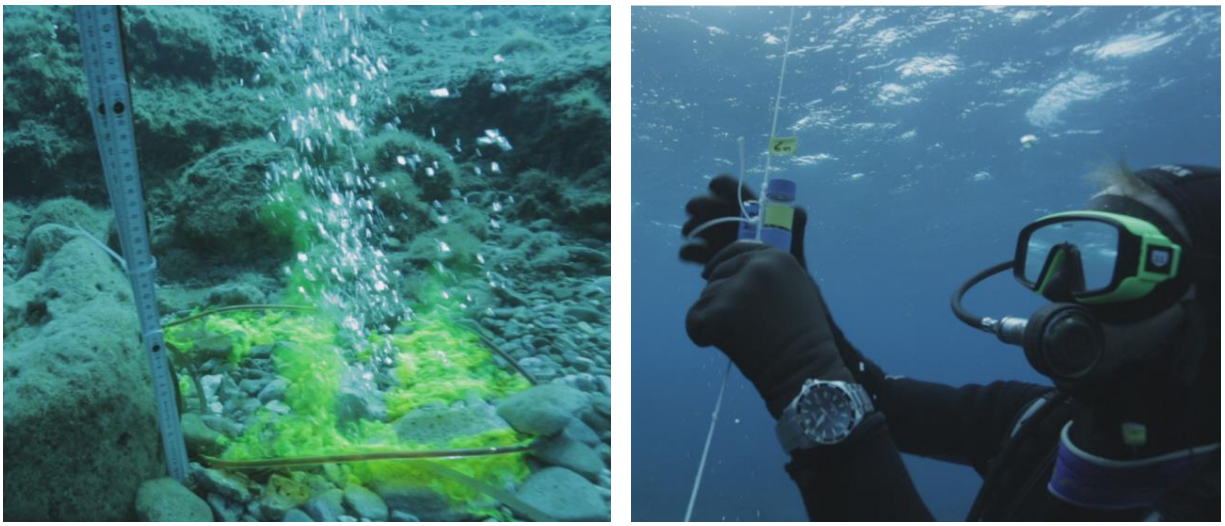

Fig. 30: Circular fluorescene injection (left) and sampling of the dispersed dye downcurrent of the injection point (right).

Both setups allowed the visualization of bubble plume dynamics and the determination of the upwelling velocity of plume water. Experiment 2 additionally aimed at visualizing the entrainment of seawater at the base of the bubble plume. Both experiments were filmed at a rate of 240 frames per second to identify individual bubbles for rise velocity determination.

Solute Dispersion in the Near-Field of CO_2 Seepage

In addition to the visualization of bubble plume dynamics the dye release experiments at Vent C were performed to determine the rate of solute dispersion in the near-field of the seep. Therefore, 50 and 10 ml of a concentrated fluorescene-suspension was injected during the first and second experiment, respectively. Water-samples were taken 7.5, 10, 15, and 20 m downstream of the release using 40 ml clear collection vials arranged in 2 m intervals along vertical threads (Fig. 30). Surface buoys held the threads taught throughout the entire water column. Sampling was performed upwards and at intervals synchronized between the scuba divers. In total, 29 water samples were taken. Sub-samples of the injected dye and seawater samples were stored at room temperature and are currently analyzed in the home laboratory for fluorescence tracer concentrations.

Current flow measurements were done in parallel to the dye release experiments and were performed using a current meter, i.e. SonTek Argonaut S/N D338. Since the measuring principle relies on the Doppler Effect, deployment had to be in an area unaffected by bubbles, approximately 20 m NW of the seepage site. To reveal stratification of the water column 2 vertical CTD-profiles were generated before and after high winds affected the area on May 14th. A Seabird SBE 37-SM MicroCAT recorder was used for this exercise.

Preliminary Results

CTD profiling revealed no thermocline within the seepage area, neither before nor after the area was affected by the moderate gale of May 14th. However, the high winds caused an effective mixing of the entire water-column resulting in a homogeneous temperature-depth-profile (Fig. 31).

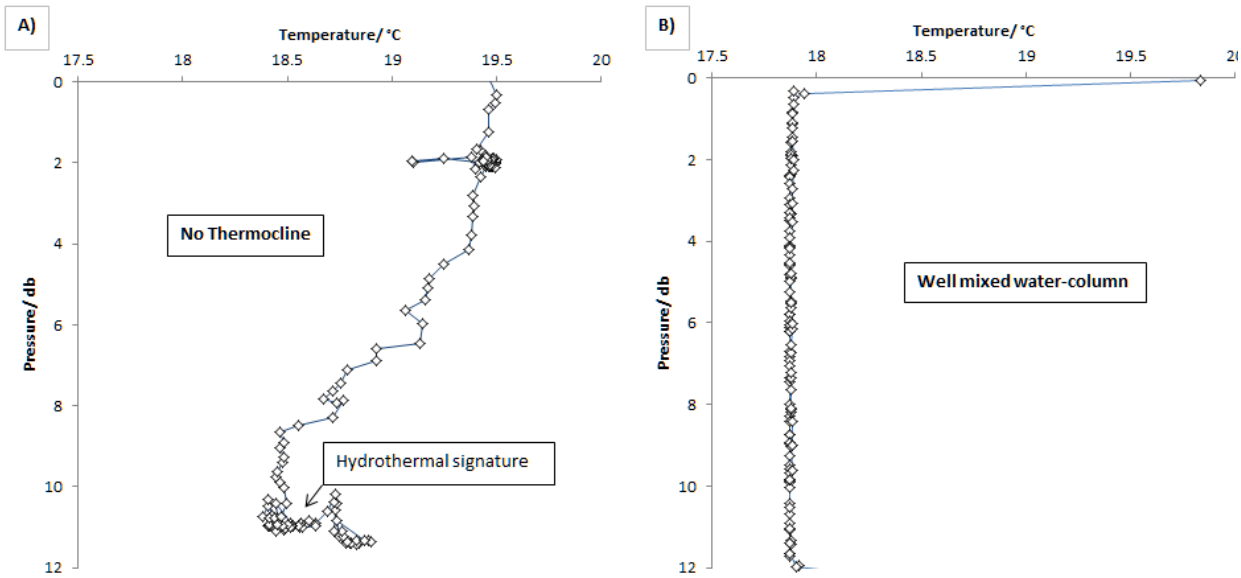

Fig. 31: The CTD profile at Bottaro Crater before high winds affected the area show no distinct thermocline, but a gradual change of T with depth until hydrothermal fluids take effect near the seafloor (A). The CTD profile after the event reveals a well-mixed water column (B).

The Argonaut was deployed before and after the moderate gale passed through, i.e. from May 11th to 13th and again from May 15th to 16th, respectively. The currents had a preferred SE-NW component at a resultant velocity ranging between 0 and 16.2 cm s^{-1}. The current direction appears to be partly correlated to the tide, at least during the first measurement-interval, where the currents showed a preferred NW and SE component during low-and high tide, respectively. However, after the May 14th, tidal control is absent, probably due to stronger winds persisting in the aftermath of the moderate gale.

Discrete gas flow measurements revealed a flux of 1.8 L min^{-1} from a location on the gravel field in the center of the crater and 9.3 L min^{-1} at Vent C, both at 12 m depth. Due to the high temporal and local variability of the gas flow from spread-out sources of the gravel field, a comparison of this number with measurements of last year's campaign is not meaningful. However, the emission rate at the discrete, marginal Vent C reported here compares to 10.7 L min^{-1} the team measured in June 2013. Since long-term, year-round data are unavailable, this discrepancy might represent natural shifts in the source strength rather than a general trend.

The images grabbed from the BPR-video display good quality with hardly any motion blur of the bubbles (Fig. 29). First video analyses of the fluorescene injection experiments indicate significant upwelling of entrained water even at low emission rates (i.e. ~ 47 cm at Vent C, ~ 19 cm/s in central gravel field). It is expected that this will have a significant effect on measured bubble rise velocities at both locations. Determination of the latter is currently in progress. Further evaluation of the data will finally allow to quantitatively determine gas bubble sizes, fluxes and the rise velocities of the bubbles themselves and the dyed ambient water.

Preliminary results of the change of the gas bubble composition emitted from central parts of the crater indicate a slow CO_2 dissolution within the lower 2 masf. Here, bubbles containing initially 93-99 Vol% of CO_2 lost less than 5 Vol% during the first 2 m of ascent. At Vent C, gas bubbles were able

to transport up-to ~30 Vol. % of their CO_2 to the sea-surface, 12 m above the seafloor. Up to 6 masf CO_2 dissolution is slow - significant CO_2 loss occurred only at higher levels (Fig. 32).

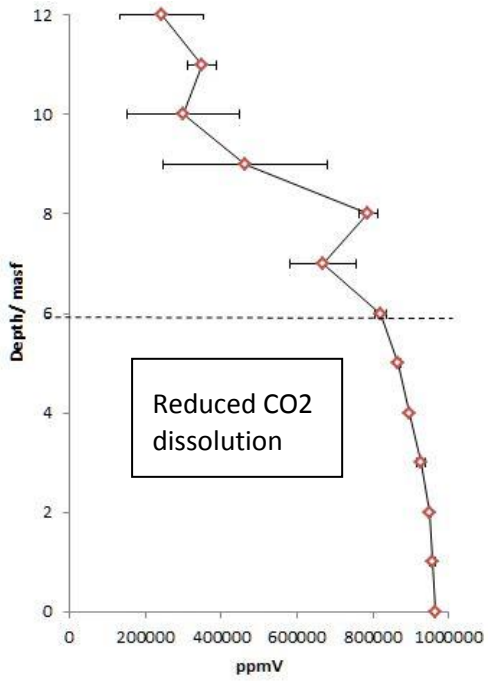

Fig. 32: CO_2 stripping from bubbles of Vent C during their rise to the sea-surface.

However, even the elevated dissolution rate at the upper levels is still not sufficient to match predictions of numerical models. Thus, the ability to transport CO_2 by bubbles is markedly enhanced with regard to model predictions (McGinnis et al., 2006) and artificially produced bubbles (Linke, 2012), where bubbles were depleted in CO_2 at faster rates and after shorter distances travelled. We hypothesize that the enhanced uprising and bubble lifetime is due to the existence of very large bubbles, highly CO_2 enriched plume water, CO_2 enriched water remaining within the crater and upwelling.

Visual inspection of video footage of the fluorescene experiments revealed that the dye rose up to 7 masf within the vent. Hence, upwelling at Vent C significantly declined midway between seafloor and sea-surface, suggesting that bubble-induced upwelling of water occurred primarily within the lower part of the water-column. In the more spread-out venting regime of the gravel field in the centre of the crater, the dye reached approximately half the rise height of Vent C, indicating upwelling was less pronounced here, certainly due to the lower bubble venting intensity. In none of the experiments the dye was visible at the sea-surface. The rise height of the dye at Vent C approximately coincides with the onset of significant stripping of CO_2 from bubbles sampled at the same site (Fig. 32), asserting the role of upwelling on transport efficiency of CO_2 via bubbles as hypothesized above.

Based on our observations and preliminary cruise results we conclude that the existing parameterizations used in numerical models are mostly applicable to simulate the dissolution of CO_2 bubble streams, in which the number flux of bubbles is not large enough to sustain the upwelling of the entrained water. At more intense vents, water entrainment and bubble-induced upwelling take control and plume hydrodynamics have to be taken into account in the modeling effort. Our data will be used to improve the parameterization used in bubble dissolution models by implementing the physics of bubble plumes.

Highlights

- The transport efficiency of CO_2 in bubble plumes is significantly higher than numerical models predict.

- Bubbles released in bubble plumes enhance the bubble lifetime, rise velocity and transport distance due to the enrichment of dissolved CO_2, and upwelling.
- In bubble plumes buoyancy appears to have a less significant effect on the bubble rise velocity, even at moderate gas emissions
- Plume induced upwelling at discrete vents of similar intensity as Vent C (approx. 10 L min^{-1}) is effective up to lower 7 m above the emission point

5 References

Aliani, S., Bortoluzzi, G., Caramanna, G., Raffa, F (2010). Seawater dynamics and environmental settings after November 2002 gas eruption off Bottaro (Panarea, Aeolian Islands, Mediterranean Sea). Cont. Shelf Res., 30, 1338-1348.

Anzidei, M., Esposito, A., Bortoluzzi, G., and Francesco De Giosa, F., 2005. The high resolution bathymetric map of the exhalative area of Panarea (Aeolian Islands, Italy). Annals of Geophysics 48, no. 6: 899-921.

Caracausi, A., Ditta, M., Italiano, F., Longo, M., Nuccio, P.M., Paonita, A., Rizzo, A. (2005). Changes in fluid geochemistry and physico-chemical conditions of geothermal systems caused by magmatic input: the recent abrupt outgassing off the island of Panarea (Aeolian Islands, Italy). Geochim. Cosmochim. Acta., 69(12), 3045-3059.

Chiocci, F. L., Bosman, A., et al. (2013). Bathy-morphological map. Eastern Aeolian Sector. Scale 1: 50 000. In: Lucchi, F., Peccerillo, A., Keller, J., Trann,. C. A. & Rossi, P. L. (eds) Geology of the Aeolian Islands (Italy). Geological Society. London. Memoirs 37: attached DVD.

Chiodini, G. and 7 others (2006) Geochemistry of the submarine gaseous emissions of Panarea (Aeolian Islands, Southern Italy): Magmatic vs. hydrothermal origin and implications for volcanic surveillance. Pure Appl. Geophys., 163, 759-780.

Dekov, V., Savelli, C. (2004) Hydrothermal activity in the SE Tyrrhenian Sea: an overview of 30 years of research. Mar. Geol., 204, 161-185.

Dickson, A. G., Sabine, C. L., Christian, J. R. (Eds.) (2007). Guide to best practices for ocean CO_2 measurements. PICES Special Publication 3, 191 pp.

Esposito., A, Giordano., G, Anzidei, M. (2006). The 2002-2003 submarine gas eruption at Panarea volcano (Aeolian Islands, Italy): Volcanology of the seafloor and implications for the hazard scenario. Marine Geology, 227, 119-134.

Italiano, F., Nuccio, P.M. (1991). Geochemical investigations of submarine volcanic exhalations to the east of Panarea, Aeolian Islands, Italy. Journal of Volcanology and Geothermal Research 46: 125–141.

Kirk, K. (2011). Natural CO_2 flux literature review for the QICS project. British Geological Survey Commissioned Report. CR/11/005: 38 pp.

Lewis, E., Wallace, D.W.R. (1998). CO2SYS—Program developed for the CO_2 system calculations. Carbon Dioxide Inf. Anal. Center; Report ORNL/CDIAC-105.

Linke, P., ed. (2012) RV Celtic Explorer EUROFLEETS cruise report CE12010 - ECO2@NorthSea: 20.07. – 06.08.2012, Bremerhaven - Hamburg GEOMAR Report, N. Ser. 004. GEOMAR, Kiel, Germany, 60 pp. DOI 10.3289/GEOMAR_REP_NS_4_2012.

Linke, P., Schmidt, M., Rohleder, M., Al-Barakati, A., Al-Farawati, R. (subm.) Novel online digital video and high-speed data broadcasting via standard coaxial cable onboard marine operating vessels. Mar. Tech. Soc. J.

Lupton, J., Lilley, M., Butterfield, D., Evans, L., Embley, R., Massoth, G., Christenson, B., Nakamura, K., Schmidt, M. (2008). Venting of a separate CO2-rich gas phase from submarine arc volcanoes – Examples from the Mariana and Tonga-Kermadec Arcs. J. Geophys. Res. 113. doi:10.1029/2007JB005467.

Mächler, L., Brennwald, M.S., Kipfer, R. (2012). Membrane inlet mass spectrometer for the quasi-continuous on-site analysis of dissolved gases in groundwater. Environ. Sci. Technol. 46, 8288-8296.

McGinnis, D. F., J. Greinert, Y. Artemov, S. E. Beaubien, and A. Wuest (2006). Fate of rising methane bubbles in stratified waters: How much methane reaches the atmosphere? Journal of Geophysical Research-Oceans, 111(C9).

McGinnis, D., Beaubien, S. E., Bigalke, N., Bryant, L. D., Celussi, M., Comici, C., De Vittor, C., Feldens, P., Giani, M., Karuza, A., Schneider von Deimling, J. (2011b). The Panarea natural CO2 seeps: fate and impact of the leaking gas (PaCO2). R/V URANIA. Cruise No. U10/2011. 27 July – 01 August 2011. Naples (Italy) – Naples (Italy) EUROFLEETS Cruise Summary Report. IFM-GEOMAR. Kiel. 55 pp. DOI 10.3289/CR_ECO2_19835.

McGinnis, D. F., Schmidt, M., DelSontro, T., Themann, S., Rovelli, L., Reitz, A., Linke, P. (2011a). Discovery of a natural CO_2 seep in the German North Sea: Implications for shallow dissolved gas and seep detection. J. Geophys. Res. 116: C03013.

Molari, M., S. Meyer, M. Weber, K. Guilini, L. Vielstädte, N. Bigalke, S. Schutting, C. Howe, M. Kreuzburg, B. Unger, M. Schneider, H. Kuhfuss, A. Eich, F. Wenzhöfer, D. de Beer, A. Ramette, C. Lott, A. Vanreusel, and A. Boetius (2013). Cruise Report ECO2-8 (Panarea Island, Italy): Effect of seabed CO2 emissions on shallow benthic microbiota (Panarea Island), cruise_report, 37 pp, Max Planck Institute for Marine Microbiology, Bremen, Germany.

Monecke, T., Petersen, S., Hannington, M. D., Anzidei, M., Esposito, A., Giordano, G., Garbe-Schönberg, D., Augustin, N., Melchert, B., Hocking, M. (2012). Explosion craters associated with shallow submarine gas venting off Panarea Island. Italy Bulletin of Volcanology 74(9): 1937-1944.

Schmidt, M., Linke, P., Sommer S., Esser D., Cherednichenko, S. (subm.) Natural CO2 seeps offshore Panarea – A test site for subsea CO2 leak detection technology. Marine Technology Society Journal.

Schneider von Deimling, J., Brockhoff, J., Greinert, J. (2007). Flare imaging with multibeam systems: Data processing for bubble detection at seeps. Geochemistry, Geophysics, Geosystems, 8(6).

Schneider von Deimling, J. and Papenberg, C. (2012) Detection of gas bubble leakage via correlation of water column multibeam images. Ocean Science, 8(2). pp. 175-181. DOI 10.5194/os-8-175-2012.

Sommer, S., Schmidt, M., Linke, P. (subm.) Continuous inline tracking of dissolved methane plume at a blow out site in the Northern North Sea UK – water column stratification impedes immediate methane release into the atmosphere. Journal of Marine and Petroleum Geology.

Walther, S. (2013) Solubility of methane in NaCl brines. A comparative analytical study using membrane inlet mass spectrometry and gas chromatography. Master Thesis, University Kiel, Kiel, 33pp.

6 Acknowledgements

We would like to express our gratitude for the excellent support by Captain Klaus Ricke and his crew provided during this cruise with RV Poseidon. Especially the professional maneuvering of a “non-differential positioning” research vessel was highly acknowledged. Furthermore, we thank the ROV team for their support during ROV operations and Sergiy Cherednichenko during cruise preparations and CTD operations. The technic and logistic center (TLZ) at GEOMAR is acknowledged for their excellent logistic support. The cruise and diving campaign has received funding from GEOMAR, the Helmholtz-Alliance "ROBEX – Robotic Exploration of Extreme Environments", the ECO2 project in the European Community's Seventh Framework Program (FP7/2007-2013) under grant agreement n° 265847, and 3 mini projects funded by the cluster of excellence “The Future Ocean”.

7 List of stations

Station No.	Gear	Date 2014	Start Time	Lat. [°N]	Long. [°E]	Depth [m]	At depth Time	Lat. [°N]	Long. [°E]	Depth [m]	End stat. Time	Lat. [°N]	Long. [°E]	Depth [m]	Remarks
569	CTD-1	04.05	06:03	38°37.148	15°05.788	85					06:47	38°37.139	15°05.802	84	Camera failure, 11 Niskin samples
570	MB-1	04.05	07:00	38°37.052	15°05.044	45					00:46	38°46.15	15°11.30	224	
571	MB-2	05.05	00:47	38°46.08	15°11.30	487					05:42	38°39.64	15°07.34	106	WCI
572	PCTD-1	05.05	06:30	38°37.108	15°05.793	78	06:37	38°37.110	15°05.788	78	07:43	38°37.57	15°05.50	63	1 TA sample
573	TA	05.05	15:34	38°38.180	15°05.395						17:00	38°40.78	15°04.10	690	
574	MB-3/MB-4	05.05	17:45	38°36.33	15°01.51	90					03:15	38°37.46	15°06.03	85	
575	MB-5/MB-6	06.05	03:15	38°37.46	15°06.03	85					05:30	38°36.88	15°05.33	104	
576	ROV-1	06.05	06:15	38°37.048	15°05.762	84					08:05				station abandoned, technical problems
577	PCTD-2	06.05	08:44	38°36.707	15°06.448	89	10:04	38°36.711	15°06.453	88	15:22	38°39.093	15°05.720	70	2 Niskin samples
578	MB-7	06.05	18:09	38°38.27	15°05.14	31					03:32	38°39.47	15°06.57	56	
579	ROV-2	07.05	06:46	38°38.636	15°05.205	42	07:11	38°38.5817	15°05.1696	44	08:52	38°38.628	15°05.151	43	Gas sample, ROV ground fault
580	ROV-3	07.05	10:44	38°38.631	15°05.152	43	11:02	38°38.6004	15°05.1686	38	15:13	38°39.210	15°05.924	69	Gas sample, 2 Niskin samples
581	MB-8	07.05	16:20	38°38.73	15°05.95	46					17:41	38°39.70	15°05.31	76	
582	MB-9	07.05	20:04	38°48.35	15°15.15						01:31	38°40.33	15°10.18	224	Stromboli
583	ROV-4	08.05	07:01	38°38.769	15°05.138	48	07:19	38°38.7699	15°05.1105	51	08:21	38°38.717	15°05.113	42	ADCP 1 deployed
584	PCTD-3	08.05	08:40	38°38.618	15°05.138	41	09:04	38°38.606	15°05.136	39	15:45	38°38.56	15°05.26	47	Grid in 3 depth layers (1m asf, 39m, 41m)
585	MB-10	08.05	16:00	38°37.81	15°02.83	60					21:10	38°36.85	15°02.60	126	West off Panarea
586	ROV-5	09.05	06:52	38°38.631	15°05.182	44	07:05	38°38.5603	15°05.1518	44	09:17	38°38.525	15°05.211	46	
587	MB-11	09.05	09:50	38°38.750	15°05.071	45					10:00	38°38.817	15°04.993	45	
588	PCTD-4	09.05	10:09	38°38.755	15°04.987	42	10:35	38°38.722	15°05.060	42	15:09	38°38.726	15°05.181	44	Grid in 3 depth layers (1m asf, 41.3m, 39.7m), 2 Niskin samples
589	MB-12	09.05	15:42	38°37.42	15°05.27	63					20:46	38°36.80	15°07.33	70	south off plateau
590	ROV-6	10.05	06:40	38°38.818	15°04.989	42	06:55	38°38.7767	15°05.0684	45	10:25	38°38.786	15°05.039	41	

Station No.	Gear	Date 2014	Start Time	Lat. [°N]	Long. [°E]	Depth [m]	At depth Time	Lat. [°N]	Long. [°E]	Depth [m]	End stat. Time	Lat. [°N]	Long. [°E]	Depth [m]	Remarks
591	PCTD-5	10.05	11:07	38°39.094	15°05.508	69	11:20	38°39.092	15°05.540	67	18:24	38°39.02	15°05.69	69	
592	MB-13	10.05	18:50	38°40.43	15°04.96	80					00:26	38°46.63	15°11.20	233	Stromboli
593	ROV-7	11.05	06:42	38°39.030	15°05.619	70	07:08	38°39.1262	15°05.6630	70	10:06	38°38.97	15°05.60	69	
594	ZODIAC	11.05	11:30	38°37.74	15°05.98	59					14:30	38°37.78	15°05.78	59	Gas and water samples at shallow vents off Botaro
595	MB-14	11.05	17:38	38°37.37	15°07.30	67					22:12	38°37.47	15°08.24	274	
596	ROV-8	12.05	07:00	38°38.793	15°05.004	74	07:13	38°38.7337	15°05.0220	74	09:46	38°38.783	15°04.992		
597	PCTD-6	12.05	10:29	38°39.096	15°05.533	72	11:03	38°39.094	15°05.550	71	14:40	38°39.092	15°05.546	71	
7598	CTD-2	12.05	14:52	38°39.060	15°05.609	75					16:05	38°39.09	15°05.63	70	11 Niskin samples
599	CTD-3	12.05	16:54	38°39.083	15°05.608	70					18:01	38°39.017	15°05.576	65	
600	MB-15	12.05	18:44	38°37.25	15°08.23	341					01:12	38°42.09	15°00.67	1538	
601	ROV-9	13.05	06:56	38°39.047	15°05.672	70	07:15	38°39.0474	15°05.5753	70	10:49	38°39.335	15°05.940	70	ADCP 2, BB, 3 Niskin samples in 2nd crater
602	PCTD-7	13.05	11:12	38°39.227	15°05.870	68	11:38	38°39.220	15°05.866	68	13:04	38°39.24	15°05.87	68	Grid had to be abandoned
603	MB-16	13.05	17:00	38°38.52	15°05.49	55					04:24	38°37.20	14°59.86	278	
604	ROV-10	15.05	11:47	38°38.714	15°05.125	40	11:55	38°38.6764	15°05.1815	41	12:17	38°38.73	15°05.11	41	Recovery of ADCP 1
605	ROV-11	15.05	13:02	38°389.085	15°05.575	67	13:17	38°39.0316	15°05.6324	67	13:59	38°38.99	15°05.61	67	Recovery of ADCP 2
606	ROV-12	16.05	09:12	38°38.757	15°05.027	40	09:14	38°38.7541	15°05.1014	41	10:27	38°38.75	15°05.00	39	Bubble box, stain release
607	CTD-4	16.05	11:18	38°38.79	15°05.05	43					12:55	38°38.78	15°04.98	40	Grid with 9 vertical casts

ROV PHOCA (ROV), Multibeam (MB), Total Alkalinity (TA), Pump-CTD (PCTD) and vertical CTD casts (CTD), time in UTC.

GEOMAR
Helmholtz-Zentrum für Ozeanforschung Kiel

GEOMAR Reports

No.	Title
1	FS POSEIDON Fahrtbericht / Cruise Report POS421, 08. – 18.11.2011, Kiel - Las Palmas, Ed.: T.J. Müller, 26 pp, DOI: 10.3289/GEOMAR_REP_NS_1_2012
2	Nitrous Oxide Time Series Measurements off Peru – A Collaboration between SFB 754 and IMARPE –, Annual Report 2011, Eds.: Baustian, T., M. Graco, H.W. Bange, G. Flores, J. Ledesma, M. Sarmiento, V. Leon, C. Robles, O. Moron, 20 pp, DOI: 10.3289/GEOMAR_REP_NS_2_2012
3	FS POSEIDON Fahrtbericht / Cruise Report POS427 – Fluid emissions from mud volcanoes, cold seeps and fluid circulation at the Don-_Kuban deep sea fan (Kerch peninsula, Crimea, Black Sea) – 23.02. – 19.03.2012, Burgas, Bulgaria - Heraklion, Greece, Ed.: J. Bialas, 32 pp, DOI: 10.3289/GEOMAR_REP_NS_3_2012
4	RV CELTIC EXPLORER EUROFLEETS Cruise Report, CE12010 – ECO2@NorthSea, 20.07. – 06.08.2012, Bremerhaven – Hamburg, Eds.: P. Linke et al., 65 pp, DOI: 10.3289/GEOMAR_REP_NS_4_2012
5	RV PELAGIA Fahrtbericht / Cruise Report 64PE350/64PE351 – JEDDAH-TRANSECT -, 08.03. – 05.04.2012, Jeddah – Jeddah, 06.04 - 22.04.2012, Jeddah – Duba, Eds.: M. Schmidt, R. Al-Farawati, A. Al-Aidaroos, B. Kürten and the shipboard scientific party, 154 pp, DOI: 10.3289/GEOMAR_REP_NS_5_2013
6	RV SONNE Fahrtbericht / Cruise Report SO225 - MANIHIKI II Leg 2 The Manihiki Plateau - Origin, Structure and Effects of Oceanic Plateaus and Pleistocene Dynamic of the West Pacific Warm Water Pool, 19.11.2012 - 06.01.2013 Suva / Fiji – Auckland / New Zealand, Eds.: R. Werner, D. Nürnberg, and F. Hauff and the shipboard scientific party, 176 pp, DOI: 10.3289/GEOMAR_REP_NS_6_2013
7	RV SONNE Fahrtbericht / Cruise Report SO226 – CHRIMP CHatham RIse Methane Pockmarks, 07.01. - 06.02.2013 / Auckland – Lyttleton & 07.02. – 01.03.2013 / Lyttleton – Wellington, Eds.: Jörg Bialas / Ingo Klaucke / Jasmin Mögeltönder, 126 pp, DOI: 10.3289/GEOMAR_REP_NS_7_2013
8	The SUGAR Toolbox - A library of numerical algorithms and data for modelling of gas hydrate systems and marine environments, Eds.: Elke Kossel, Nikolaus Bigalke, Elena Piñero, Matthias Haeckel, 168 pp, DOI: 10.3289/GEOMAR_REP_NS_8_2013
9	RV ALKOR Fahrtbericht / Cruise Report AL412, 22.03.-08.04.2013, Kiel – Kiel. Eds: Peter Linke and the shipboard scientific party, 38 pp, DOI: 10.3289/GEOMAR_REP_NS_9_2013
10	Literaturrecherche, Aus- und Bewertung der Datenbasis zur Meerforelle (*Salmo trutta trutta L.*) Grundlage für ein Projekt zur Optimierung des Meerforellenmanagements in Schleswig-Holstein. Eds.: Christoph Petereit, Thorsten Reusch, Jan Dierking, Albrecht Hahn, 158 pp, DOI: 10.3289/GEOMAR_REP_NS_10_2013
11	RV SONNE Fahrtbericht / Cruise Report SO227 TAIFLUX, 02.04. – 02.05.2013, Kaohsiung – Kaohsiung (Taiwan), Christian Berndt, 105 pp, DOI: 10.3289/GEOMAR_REP_NS_11_2013

GEOMAR
Helmholtz-Zentrum für Ozeanforschung Kiel

No.	Title
12	RV SONNE Fahrtbericht / Cruise Report SO218 SHIVA (Stratospheric Ozone: Halogens in a Varying Atmosphere), 15.-29.11.2011, Singapore - Manila, Philippines, Part 1: SO218- SHIVA Summary Report (in German), Part 2: SO218- SHIVA English reports of participating groups, Eds.: Birgit Quack & Kirstin Krüger, 119 pp, DOI: 10.3289/GEOMAR_REP_NS_12_2013
13	KIEL276 Time Series Data from Moored Current Meters. Madeira Abyssal Plain, 33°N, 22°W, 5285 m water depth, March 1980 – April 2011. Background Information and Data Compilation. Eds.: Thomas J. Müller and Joanna J. Waniek, 239 pp, DOI: 10.3289/GEOMAR_REP_NS_13_2013
14	RV POSEIDON Fahrtbericht / Cruise Report POS457: ICELAND HAZARDS Volcanic Risks from Iceland and Climate Change:The Late Quaternary to Anthropogene Development Reykjavík / Iceland – Galway / Ireland, 7.-22. August 2013. Eds.: Reinhard Werner, Dirk Nürnberg and the shipboard scientific party, 88 pp, DOI: 10.3289/GEOMAR_REP_NS_14_2014
15	RV MARIA S. MERIAN Fahrtbericht / Cruise Report MSM-34 / 1 & 2, SUGAR Site, Varna – Varna, 06.12.13 – 16.01.14. Eds: Jörg Bialas, Ingo Klaucke, Matthias Haeckel, 111 pp, DOI: 10.3289/GEOMAR_REP_NS_15_2014
16	RV POSEIDON Fahrtbericht / Cruise Report POS 442, "AUVinTYS" High-resolution geological investigations of hydrothermal sites in the Tyrrhenian Sea using the AUV "Abyss", 31.10. – 09.11.12, Messina – Messina, Ed.: Sven Petersen, 32 pp, DOI: 10.3289/GEOMAR_REP_NS_16_2014
17	RV SONNE, Fahrtbericht / Cruise Report, SO 234/1, "SPACES": Science or the Assessment of Complex Earth System Processes, 22.06. – 06.07.2014, Walvis Bay / Namibia - Durban / South Africa, Eds.: Reinhard Werner and Hans-Joachim Wagner and the shipbord scientific party, 44 pp, DOI: 10.3289/GEOMAR_REP_NS_17_2014
18	RV POSEIDON Fahrtbericht / Cruise Report POS 453 & 458, "COMM3D", Crustal Structure and Ocean Mixing observed with 3D Seismic Measurements, 20.05. – 12.06.2013 (POS453), Galway, Ireland – Vigo, Portugal, 24.09. – 17.10.2013 (POS458), Vigo, Portugal – Vigo, Portugal, Eds.: Cord Papenberg and Dirk Klaeschen, 66 pp, DOI: 10.3289/GEOMAR_REP_NS_18_2014

For GEOMAR Reports, please visit:
https://oceanrep.geomar.de/view/series/GEOMAR_Report.html

Reports of the former IFM-GEOMAR series can be found under:
https://oceanrep.geomar.de/view/series/IFM-GEOMAR_Report.html

GEOMAR
Helmholtz-Zentrum für Ozeanforschung Kiel

Das GEOMAR Helmholtz-Zentrum für Ozeanforschung Kiel
ist Mitglied der Helmholtz-Gemeinschaft
Deutscher Forschungszentren e.V.

The GEOMAR Helmholtz Centre for Ocean Research Kiel
is a member of the Helmholtz Association of
German Research Centres

Helmholtz-Zentrum für Ozeanforschung Kiel / Helmholtz Centre for Ocean Research Kiel
GEOMAR
Dienstgebäude Westufer / West Shore Building
Düsternbrooker Weg 20
D-24105 Kiel
Germany

Helmholtz-Zentrum für Ozeanforschung Kiel / Helmholtz Centre for Ocean Research Kiel
GEOMAR
Dienstgebäude Ostufer / East Shore Building
Wischhofstr. 1-3
D-24148 Kiel
Germany

Tel.: +49 431 600-0
Fax: +49 431 600-2805
www.geomar.de